Planetary geomorphology

Susan J. Conway

History of the Study of Landforms Volume 5: Geomorphology in the Second Half of the Twentieth Century

Section C: Advances in research on processes and landforms

Chapter 25: Planetary geomorphology

Susan J. Conway

Nantes Université, Université d'Angers, Le Mans Université, CNRS UMR 6112 Laboratoire de Planétologie et Géosciences, France

Abstract

With the advent of the space age, planetary geomorphology has become a stand-alone discipline. This contribution provides a summary of the different processes that have been identified to form landscapes and landforms on planetary bodies in our Solar System, including rocky planets, icy planets and moons, dwarf planets, comets and asteroids. I highlight the insights these landforms have provided into the workings of these bodies and how what has been learnt in space has often taught us new lessons about the Earth. Finally, I conclude that despite the limitations imposed by remote sensing, planetary geomorphology has a bright future in planning future missions to explore our Solar System as well as understanding the data that will be returned.

1 Introduction

This chapter is rather different from the rest of those in this book. First it is the only one that takes us away from our own planet. Secondly, it deals with a topic that was not covered, for obvious historical reasons, in the four previous volumes of the History of the Study of Landforms. Thirdly, it does not restrict itself to the temporal span of 1965-2000 which is the focus of this book. It reviews progress in the study of planetary geomorphology up until the present and shows the progress that has been made since the first successful missions were carried out from the mid-1960s onwards - It was in 1965 that Mariner 4 brought us back the first close-up photographs of another planet: Mars.

Planetary geomorphology is a branch of planetary science, which was born in the second half of the Twentieth Century from astronomy and has foundations in geology, meteorology, chemistry and biology. The rise of planetary geomorphology as a discipline goes hand in hand with an increasing use of satellite remote sensing data to study our own planet and the associated development of techniques to exploit these data.

The first remote sensing image of the Earth taken from space was in 1946. Only twenty years later, the NASA Mariner missions marked the first of a flurry of space missions that have only increased in number as the century progressed, bringing us images, topography and other data from all the major bodies in the Solar System and more. The objective of this chapter is not to provide a history of space exploration, which is done elsewhere (e.g., Burns, 2010), but to highlight the main discoveries and associated advances in the understanding of the processes and landforms of other worlds spanning the era of robotic and human exploration of space.

In order for landscapes and landforms to be studied the surface of the body has to be resolved at a sufficient resolution (in the author's opinion at least hundreds of metres per pixel). Hence to date, planetary geomorphology is restricted to solid bodies in our Solar System and relies on space probes sent to or near to the body of interest. We therefore have geomorphological information on (listed in approximate increasing solar distance):

- Mercury
- Venus*
- The Moon*
- Mars* and its moons Phobos and Deimos
- Dwarf planet Ceres in asteroid belt
- Asteroids (Bennu*, Ryugu *, Itokawa*, Vesta, Ida, Eros, Mathilde, Gaspra, Šteins, Toutatis)
- The satellites of Jupiter (Io, Europa, Ganymede, Callisto)
- The satellites of Saturn (Pan, Daphnis, Atlas, Prometheus, Pandora, Epimetheus, Janus, Mimas, Enceladus, Tethys, Telesto, Calypso, Dione, Helene, Rhea, Titan*,Hyperion, Iapetus, Phoebe)
- The satellites of Neptune (Proteus, Triton)
- The satellites of Uranus (Miranda, Ariel, Umbriel, Titania, Oberon)
- Dwarf planet Pluto and its moon Charon
- Trans-Neptunian Kuiper belt object "Arrokoth"
- Comets (Tempel 1*, Churyumov–Gerasimenko 67P*, Borrelly, Wild 2, Hartley 2)

(A * symbol indicates a landed mission)

This exploration has revealed a suite of familiar and unfamiliar processes and landforms compared to those found on Earth. This review will consider first processes and landforms already known from studying the Earth before the space exploration era and then move towards those processes and landforms less studied before Planetary Geomorphology became a distinct subdiscipline. Each section will highlight lesser-known landforms and knowledge gained from studying other worlds. For an exhaustive list of the landforms present on other worlds I refer the reader to the Encyclopaedia of Planetary Landforms (Hargitai and Kereszturi, 2015). For brevity only one or two references are cited per topic, with the intent that an interested reader can use them to access to the wider relevant literature on each topic.

2 Planetary aeolian landforms and processes

All bodies with an atmosphere have wind and aeolian landforms have been reported from: Mars, Venus Titan and Pluto (Lorenz and Zimbelman, 2014; Telfer et al., 2018), as well as of course Earth. For a full review of planetary aeolian landforms and associated processes I refer interested readers to Bourke et al. (2019). The observation of aeolian bedforms including ripples, megaripples and dunes on other planetary bodies (Figure 1a,b) has been very important for understanding the basic physics underlying aeolian processes, because these planetary bodies provide different atmospheric densities and particle densities spanning a wider range of parameter space than accessible on Earth at the landscape-scale (Kok et al., 2012; Lapôtre et al., 2020). Martian aeolian bedforms have a wider diversity of form and size than their terrestrial equivalents (e.g., Bourke, 2010; Sullivan et al., 2020), which has led to researchers to question whether the basic physics underlying their formation are indeed the same. A prime example is the landform called a Transverse Aeolian Ridge (Figure 1c) which at < 1 m tall are thought to represent megaripples whose morphology is determined by grainsize sorting rather than reptation and creep and whose origin remains unknown at larger

amplitudes (Zimbelman and Foroutan, 2020). Another example comes from radar images of longitudinal parallel and occasionally bifurcating ridges have been interpreted to be longitudinal dunes (Figure 1d) on Venus and Titan. Such dunes on Earth indicate strongly unimodal winds yet the "physics of saltation on Titan and Venus is fundamentally different from that on Earth and Mars […] dominated by direct fluid lifting" (Kok et al., 2012).

Hence, planetary observations have also revealed aeolian processes that are only experienced on extra-terrestrial environments resulting in potentially unique landforms. These include bedforms created by ablation (in the form of sublimation of ices – see also Section 11) rather than particle movements (Bordiec et al., 2020), which have so far only been studied in detail on the Antarctic ice cap (van den Broeke and Bintanja, 1995) or in ice caves (Obleitner and Spötl, 2011). Another surprising result was the discovery of dunes on the comet 67P Churyumov–Gerasimenko, which has no atmosphere (Jia et al., 2017; Thomas et al., 2015). These "dunes" are thought to form at times when the comet is close to the sun causing vigorous outgassing and strong winds being setup between sunlit and shadowed areas on the surface (Jia et al., 2017). Scouring "upwind" and build-up of sediment on the "downwind" of boulders supports this hypothesis (Mottola et al., 2015).

Abrasion by particles lofted by the wind results in erosional aeolian landforms, such as yardangs and the landscape-scale (Figure 1e) and ventifacts at the "field" scale (e.g., Wells and Zimbelman, 1997) – the orientation of these landforms is used as an important indicator of prevailing wind directions. Yardangs have been studied in most detail on Mars, but also have been suggested on Venus (Greeley et al., 1995), Titan (Paillou et al., 2016) and as an alternative interpretation of the "dunes" on Pluto (Moore et al., 2018). The study of yardangs on Mars drove a renaissance for their study on Earth (Goudie, 2007) where their climate significance is still debated. Ventifacts have been observed at the surface of Mars and are remarkably similar to those found on Earth (Knight, 2008; Laity and Bridges, 2009) and most modern studies of terrestrial ventifacts refer to planetary-driven research on this topic.

Wind can also drive the formation of inverted landforms, which have been of particular importance in revealing ancient fluvial processes on Mars (Davis et al., 2016; Day and Kocurek, 2016)(Section 3). Wind is the agent that erodes and deflates the sediments surrounding the channel(s) which are more resistant to abrasion (Figure 1e). This additional resistance can come about from cementation, coarser grainsizes or lava capping (e.g., Williams et al., 2009).

Particular to Mars are landforms related to the copious dust at its surface, which also influences the atmospheric circulation on that body (e.g., Madeleine et al., 2011). Dust via airfall is incorporated in sedimentary deposits and ice-deposition landforms (e.g. the polar caps - Kieffer, 1990; or the ice-dust latitude dependant mantle - Mustard et al., 2001). Unique to Mars are "Slope Streaks" which are landforms associated with dust motion down steep slopes (e.g., Schorghofer et al., 2007; Sullivan et al., 2001), see Section 7 for further details. Dust Devils are atmospheric vortices which are common on Mars (Figure 1f) and have been observed by every landed mission (e.g., Ferri et al., 2003; Greeley et al., 2006b; Ryan and Lucich, 1983; Thomas and Gierasch, 1985). They can also be found in deserts on Earth (Balme and Greeley, 2006), yet on Mars they often remove the dust on the surface leaving a tortuous track in their wake which is clearly visible from orbit. Much recent research on terrestrial dust devils has been driven by the desire to better understand the phenomenon on Mars (e.g., Balme et al., 2012; Reiss et al., 2010).

3 Planetary fluvial landforms and processes

The possibility of extraterrestrial fluvial geomorphology was first revealed by the discovery of valley networks and channel systems on the surface of Mars (Masursky, 1973) (Figure 2a). On Saturn's satellite Titan fluvial landforms in the form of valley networks (Porco et al., 2005; Tomasko et al., 2005) are thought to be formed by flowing liquid methane eroding the 'bedrock' of ice (Perron et al., 2006) (Figure 2b). Together with the observation of lakes (see section 4), the existence of valley networks on Titan has led to the hypothesis of a hydrocarbon-cycle driven by the decade-long seasonal cycle and atmospheric synthesis of hydrocarbons. On Venus, the river-like canali could be lava channels or carved by, another as-yet unidentified, fluid (Jones and Pickering, 2003; Kargel et al., 1994; Komatsu and Baker, 1994). Equally dendritic valleys on Pluto have been proposed to be carved by flowing liquid nitrogen (Stern et al., 2017) - the favoured alternate interpretation as glacial in origin, is described in Section 8.

The observation of valley networks motivated the hypothesis that Mars had a full-hydrological cycle early in its history, when its atmospheric density was higher allowing surface liquid water to be stable (Baker et al., 1991; Pollack et al., 1987). This valley networks are visible in a degraded (Ansan et al., 2008; Baker and Partridge, 1986) or inverted (Davis et al., 2016) state on the oldest visible surfaces of Mars (Figure 2a). Some of these valleys have low tributary order/number and by analogy with valleys with similar morphology on Earth have been interpreted to originate via groundwater sapping (Luo and Howard, 2008), hence revealing the potential presence of aquifers, although this interpretation has been questioned (Lapotre and Lamb, 2018). Some have also been interpreted to originate from sub-icesheet drainage (Grau Galofre et al., 2020), attesting to potentially widespread glaciation early in Mars' history (Fastook and Head, 2015). The observation of meandering channel belts on Mars brought into question the hypothesis that vegetation was a prerequisite for developing meanders early in Earth's history (Ielpi and Lapôtre, 2020).

Outflow channels on Mars – thought to represent colossal outbursts of water (Baker and Kochel, 1979) from pressurised aquifers (Marra et al., 2015) - reach hundreds of kilometres in width and thousands in length (Figure 2c). They are characterised by streamlined obstacles and often multiple terrace levels indicating several pulses of activity (Warner et al., 2009). The outflow channels often originate at "Chaos Terrain" which also exists on Mercury (Rodriguez et al., 2020), Europa and Pluto (Skjetne et al., 2021) (Figure 2d), and hence is not a landform directly connected to fluvial processes. Chaos terrain is thought to form by the fracturing of a layer of crust sliding over a lower lubricated layer (water in the case of Mars and Europa and glacial flow of N_2 ice for Pluto). Alternatively, such outflow channels could be carved by very fluid lava (Leverington, 2011), as is thought to be the case for analogous channels found on Mercury (Byrne et al., 2013).

Mars' surface hosts many enigmatic discontinuous channel segments, some of which have been related to water release by impacts (Mangold, 2012). Others terminate in landforms that resemble alluvial fans on Earth, such as Peace Vallis and its fan that was explored by the Curiosity Rover and found to contain conglomerates (Williams et al., 2013). These observations, together with those of the outflow channels point to surface water occurring only episodically, which contrasts with the older valley networks which point to a full-hydrological cycle having existed on Mars. As surface liquid water is not thought to have been stable for the last 1 Ga due to low atmospheric pressure and humidity, all together this points to Mars's surface becoming more arid over time.

The smallest planetary landforms thought to be related to fluvial activity are kilometre-scale martian gullies (Figure 2e) (Conway et al., 2019; Malin and Edgett, 2000) and the metres-wide and up to hundreds of metres long Recurring Slope Lineae or "RSL" on Mars (Figure 2f) (McEwen et al., 2011).

Martian gullies resemble first-order drainage systems dominated by debris flow processes on Earth, yet present-day flows in martian gullies during local winter argue against a completely fluvial origin (Diniega et al., 2010; Dundas et al., 2019) – see Section 11. RSL are low albedo streaks that grow in the hottest times of year extending from rocky steep slopes (Ojha et al., 2014) and have been suggested to be water or brine seeps (Stillman et al., 2020), however the temporal and spatial limits of orbital observations mean their origin remains enigmatic and could represent a uniquely martian surface process and landform (F. Schmidt et al., 2017).

4 Coastal, lacustrine and karstic processes and landforms

Mars is the only planet besides Earth in the Solar System which is suspected to have had ocean-scale open bodies of standing liquid (in this case water). Mars' valley networks and outflow channels generally terminate in the northern lowlands and it is around these plains that two or more levels of putative shorelines have been identified (Carr and Head, 2019; Parker et al., 1993). These shorelines are characterised by a continuously traceable contact (expressed by albedo and/or topographic contrasts - Figure 3a) over thousands of kilometres and interpreted to represent wavecut platform(s). The lack of features typically associated with paleoshorelines on Earth, such as terraces, or barrier ridges (Ghatan and Zimbelman, 2006; Malin and Edgett, 1999), means this interpretation remains contentious. Variations in their altitude have been attributed to tectonic deformation post-formation (Citron et al., 2018), and are also used as evidence against the landforms representing shorelines (Sholes et al., 2021). The evidence for an ancient ocean is bolstered by the presence of deltas whose altitudes are consistent with the ocean levels represented by the shorelines (Di Achille and Hynek, 2010). Some of the shoreline landforms are alternately interpreted as the wash-up deposits of tsunamis (Figure 3b) (Costard et al., 2017; Rodriguez et al., 2016), which also implies the presence of an ocean.

Deltas are also one of the key lines of evidence in favour of the prevalence of paleolakes on ancient Mars (Mangold et al., 2012) (Figure 3c). Other lines of evidence include sedimentary and in situ observations by the Mars Science Laboratory rover Curiosity (Stein et al., 2018), spectral observations from orbit (Dehouck et al., 2010), and morphological arguments – e.g., channels ingress into depressions, but have no outlet or a higher elevation outlet (Cabrol and Grin, 1999; Fassett and Head III, 2008; Goudge et al., 2016, 2015). The only other body in the Solar System thought to host (or have hosted) seas or lakes is Saturn's Moon Titan (Figure 3d), whose 1.5 bar nitrogen-dominated atmosphere and -180°C surface temperature means that liquid methane is believed to be the main constituent of these lakes or seas, which are mainly located in polar regions. While some of these bodies are connected to drainage systems, others are thought to be the result of karstic-type dissolution processes (Mastrogiuseppe et al., 2019). Deposits interpreted to be evaporitic associated with basins located at Titan's tropics are inferred to be paleolakes or paleoseas (Moore and Howard, 2010), which could have resulted from seasonal (decadal timescales) or longer-term climatic changes on Titan (MacKenzie et al., 2014).

Numerous sulphate salt deposits exist on Mars and hundred-metre-scale depressions within them have been linked to karstic processes (Baioni and Sgavetti, 2013; Sefton-Nash et al., 2012) potentially related to groundwater circulation (Grindrod and Balme, 2010). Dissolution has been invoked to partly explain the collapse features associated with chaos terrain (described in Section 3). Pseudokarst is where material is lost by mechanisms other than dissolution e.g. thermokarst, which in a planetary context has been employed to describe karst-like features caused by temperature induced volatile loss in contrast to the terrestrial definition which involves melting of ice-rich permafrost. These karstic landforms are described further in Section 11 and martian thermokarst initially also attributed to melting ice-rich permafrost are referred to in Section 8).

5 Planetary tectonic landforms and processes

Tectonic landforms are ubiquitous on planetary surfaces. Even the smallest bodies that have been explored, such as comets, show signs of fracturing which result from interior forces (El-Maarry et al., 2015). However, only the Earth has plate tectonics, whose action profoundly influences its landscapes, making it one of the most dynamic surfaces in the Solar System. Europa, which is an icy Moon of Jupiter, may have an analogous system of plates, but in this case the plates are made of water ice floating on a liquid water "mantle" (Kattenhorn and Prockter, 2014) (Figure 4a). The detailed morphology of Europa's plates was key in motivating the dynamic modelling that underpins our understanding of this planet's interior. A similar "jostling plates" model has been advanced for Venus based on analogy with deformational structures observed in actively deforming contents on Earth (Byrne et al., 2021). Typical compressional tectonic landforms include wrinkle ridges, high relief ridges and lobate scarps (Figure 4b, c), common on Mercury (Byrne et al., 2014), Mars (Herrero-Gil et al., 2019; Nahm and Schultz, 2011), and the Moon (Schleicher et al., 2019; Watters et al., 2010). They are thought to be compound landforms representing folds above faults, but not common on Earth (Crane, 2020) hampering their interpretation. Global mapping these compressional tectonic features on Mercury has provided an independent estimate of its global contraction (Byrne et al., 2014).

Typical extensional forms include graben (Figure 4d) and are found commonly throughout the solar system. Graben systems are sometimes associated with pit-chains, which are thought to be caused by fracture dilation (Ferrill et al., 2011) (Figure 4e) and whose origin is also interpreted to be magmatic (see section 6):

Extensional tectonic features are very common on the icy moons of Jupiter, Saturn, and Neptune and their patterns have been vital in understanding the forces that influence these bodies including tidal stresses from their planets, crustal thickness, and mantle motions (Collins et al., 2009). Tectonic landforms on these icy satellites can be unique, for example the double ridges on Europa (Figure 4a), or the twisting double ridge-sets on Triton, or the prominent single equatorial ridge on Iapetus (Figure 4f).

6 Planetary volcanic landforms and processes

The definition of volcanism has been extended beyond magmatic volcanism in a planetary science context, to include also sedimentary volcanism and cryovolcanism and each are thought to produce somewhat distinct landforms. Magmatic volcanism requires interior heating and an availability of silicates to produce magma, so generally related volcanic landforms are found on terrestrial planets of the inner solar system, as well as Earth's Moon and Jupiter's innermost moon Io. Volcanism at the largest scale (hundreds to thousands of kilometres) is recognised in the form of volcanic constructs, such as Tuulikki Mons on Venus (Basilevsky et al., 2012) (Figure 5a) or Olympus Mons on Mars (Morris, 1982) and/or volcanic plains, such as the Mare of the Moon (Figure 5b) (Stuart-Alexander and Howard, 1970) or the Northern Plains of Mercury (Denevi et al., 2013). Peculiar to Venus are coronae, arachnoids and novae, which are large patterns of fractures (concentric, concentric-radial and radial, respectively) believed to be volcanic in origin (Head et al., 1992). Io is the only planetary body in the Solar System where volcanic eruptions have actually been observed occurring (McEwen, 1998).

Recognisable at the kilometre to tens of kilometre-scale on Mars, the Moon, Venus and Io are individual lava flows (Figure 5c – io "dark flow") and lava channels. On the Moon sinuous rilles (Figure 5d) – sinuous channels hundreds of metres to kilometres in width and up to 500 km long - were initially attributed to water (Peale et al., 1968), but are now generally acknowledged to be lava channels carved predominantly by thermal erosion (Hurwitz et al., 2013). "Skylights" (Figure 5e) –

deep nearly vertically walled circular to elliptical depressions – on Mars and the Moon are interpreted to represent the collapse of the roof of lava tubes and present considerable interest as natural habitats which could be exploited for human exploration (Sauro et al., 2020). Larger pit chains are thought to represent collapse on the withdrawal of lava from dikes (Wyrick, 2004) but could also be tectonic in origin (see Section 5).

Evidence for explosive volcanism is usually smaller-scale (tens of kilometres) and more subtle in its surface expression, taking the form of pits with associated red-colouration on Mercury (Kerber et al., 2011) (Figure 5f), low-albedo markings on the Moon (Gustafson et al., 2012) and km-scale volcanic cones on Mars (Brož and Hauber, 2012).

Sedimentary volcanism (often called mud volcanism) is driven by the circulation of water through a planetary crust generally driven by tectonic forces or density contrasts and has been reported on Mars (Figure 6a). Here, movement of groundwater is thought to have remobilised ancient sedimentary deposits creating pitted cones and lobate-fronted flow features (Oehler and Allen, 2010). On Earth, mud volcanoes are the most commonly expressed landform resulting from sedimentary volcanism and differ from their volcanic counterparts in terms of morphology, however this distinction is harder to make on other bodies because of differences in environmental conditions are difficult to directly infer the potential morphologic impacts (Brož et al., 2020).

Cryovolcanism is thought to be more abundant in the icy moons of the outer planets (Ahrens, 2020; Kargel, 1995), where liquid water and ice, are thought to substitute almost directly the more familiar lava and silicic rocks in the functioning of the volcanic plumbing system. On Ceres, brine driven cryovolcanism is thought to explain the bright faculae, such as Cerealia Facula in Occator Crater (Nathues et al., 2020) (Figure 6b). Inspired by planetary research cryovolcanic processes have been cited as a potential cause for explosive pits that occurred in continuous permafrost on the Yamal Peninsula in Russia (Buldovicz et al., 2018).

Diapirism (either compositional or thermal), where a less dense material rises through a denser one above it is often associated with sedimentary- or cryo-volcanism. The resulting landforms can be a result of tectonic deformation rather than extrusion at the surface. Several enigmatic terrains have been attributed to diapirism or associated convection: the honeycomb and banded terrain in Hellas basin on Mars (Figure 6c - cassis) (Bernhardt et al., 2016), Cantaloupe terrain on Triton (Schenk and Jackson, 1993) or the cellular structure of Sputnik Planitia on Pluto (Howard et al., 2017b) (Figure 6d).

7 Mass movements on planetary bodies

Landslides have been identified on nearly every solid planetary surface observed in the solar system. Notably the long runout landslides observed on bodies as diverse as Mars (Crosta et al., 2018; McEwen, 1989), Mercury (Brunetti et al., 2015), the Moon (Boyce et al., 2020), Iapetus (Singer et al., 2012), Callisto (Moore et al., 1999), Pluto's moon Charon (Beddingfield et al., 2020), Ceres (Duarte et al., 2019) and Comet 67P (Lucchetti et al., 2019) (Figure 7a-c, landslide on Ceres, callisto moore et al, Mars, Mercury) have inspired a comparative planetology approach seeking to understand the physical processes underlying the motion of the long-runout landslides. The role that volatiles do or do not play in the mobility of landslides is a key recurring theme. On one hand being used as an argument to support inclusion of volatiles on Iapetus (Singer et al., 2012) and on the other being used to refute their action on comet 67P (Lucchetti et al., 2019). For Ceres (Johnson and Sori, 2020; B. E. Schmidt et al., 2017) as for Mars, both cases have been presented and no consensus has yet been achieved (Harrison and Grimm, 2003; Johnson and Campbell, 2017).

Peculiar to Mars are a landform called “Slope Streaks” (Figure 7d) (Sullivan et al., 2001), which are thought to represent avalanches of dust-sized material, taking the form of contrasting albedo, downslope-widening streaks, up to several kilometres in length and hundreds of metres wide. Slope Streaks usually appear as relatively dark (and sometimes relatively light) downslope oriented streaks with barely detectable or negligible relief (Brusnikin et al., 2016; Chuang et al., 2007), which fade to the background albedo over time. They often widen from a point source and can be sinuous, overcome obstacles and have digitate margins. They can overtop small obstacles (Brusnikin et al., 2016) yet are generally diverted by topographic irregularities (Miyamoto, 2004), so can form complex bifurcating features. The involvement of liquid water has been invoked to explain their mobility on low slopes (Bhardwaj et al., 2017), but dry granular mechanisms seem to also provide an adequate explanation (Dundas, 2020).

Images at better than 1 m/pix on the Moon have revealed a diversity of mass movements on steep slopes, including lobate and digitate dry granular flows on Moon (Figure 7e,f) (Senthil Kumar et al., 2013; Xiao et al., 2013). The Moon and Mercury host unique surface textures hinting at slower downslope movement of the surface regolith, including “elephant hide texture” on the Moon and “chevron texture” on Mercury, whose precise origin is unknown (Zharkova et al., 2020). On Mars, tens to hundreds of metre-scale lobate forms on slopes have been associated with the existence of a solifluction-type movement on Mars (Gastineau et al., 2020; Johnsson et al., 2012) and are found in association with other landforms interpreted to be periglacial in origin (see Section 8).

8 Planetary glacial and permafrost landforms and processes

Mars has an extensive suite of landforms at its mid-latitudes which are commonly accepted to be debris covered glaciers (Figure 8a) dating from the last 1 Ga of Mars’ history. These glaciers can cover tens to hundreds of kilometres and reach hundreds of metres thick. Their water ice core has been revealed through orbital radar sounding (Petersen et al., 2018; Plaut et al., 2009), and their surface textures indicate slow viscous deformation. Modelling studies (Karlsson et al., 2015; Parsons et al., 2011) and the general lack of landforms associated with melt imply that the ice is likely perennially frozen to the glacier bed (cold-based glaciers). The rare discovery of ridges interpreted to be eskers connected to extant glaciers suggests that this constraint is only occasionally overcome (Butcher et al., 2020; Gallagher and Balme, 2015). Isolated eskers and moraine-like ridges have been interpreted to be signs of ancient glaciation and/or icesheets (Butcher et al., 2016; Head and Marchant, 2003).

On Pluto the existence of glaciers of N_2 ice has been reported (Howard et al., 2017a). These take the form of smooth material filling topographic lows in highland terrains with longitudinal albedo lineations indicating flow direction, which appear to flow out onto Sputnik Planum at lower elevation where the lineations blend into the plains materials (Figure 8b). These glaciers are hundreds of kilometres in length. The only other planetary body where debris covered glaciers have been proposed is the dwarf planet Ceres (B. E. Schmidt et al., 2017), but their ambiguous morphology means that landsliding could also be a viable interpretation.

Permafrost conditions exist on many bodies, particularly those in the outer solar system, yet landforms typically associated with permafrost on Earth generally imply the degradation of ground ice, or at least cycling of temperatures near water’s triple point to produce terrain modifications e.g., periglacial landforms. One exception is the formation of polygon crack patterns in ice-rich soil by thermal contraction, which only requires temperature cycling – metre to decametre-scale examples of these landforms have been widely reported at latitudes greater than 50°N and S on Mars (Mangold, 2005; Mellon et al., 2009) where ground ice is thought to be prevalent (Feldman et al., 2011). Periglacial landforms have been reported on Mars, implying the action of freeze-thaw cycling

in the planet's recent history and hence their interpretation as such remains a subject of debate. These landforms include:

- Gullies, which are alcove-channel-fan systems hundreds of metres to kilometres in length, which are found on steep slopes in the mid to high latitudes on Mars (Figure 2e) (Harrison et al., 2015; Malin and Edgett, 2000). Their resemblance at landscape and landform-scale to gullies carved by overland-flow and debris flow on Earth means that they have been widely interpreted to form by these processes (Balme et al., 2006; Conway and Balme, 2016; de Haas et al., 2015), and the source of water is likely from snow and/or ground ice thaw. Yet their present activity has led to a re-evaluation of this interpretation (see Section 11 - Sublimation landforms and processes).
- Surface albedo and/or clast patterns that resemble, and have a similar-scale to, sorted patterned ground on Earth, including sorted circles on flat ground and stripes on sloping terrain (Gallagher et al., 2011; Soare et al., 2016) (Figure 8c).
- Lobate forms interpreted to be solifluction lobes (see section 7) (Figure 8d).
- Polygonal patterned ground where the centres are lower than the margins and those margins form double-ridges implying the existence of ice wedges (Soare et al., 2021, 2014) (Figure 8e).
- Scalloped depressions (Soare et al., 2008) and polygon junction pits (Costard et al., 2016) were initially interpreted to be true thermokarst (i.e. caused by thaw). However, together with expanded craters (Viola et al., 2015) are now thought to be caused by sublimation (Dundas et al., 2015), see Section 11.
- Tens to hundreds of metre isolated hills or mounds with summit cracks/depressions interpreted to be caused by ice-heave, otherwise known as "pingos" (Burr et al., 2009; Soare et al., 2005) (Figure 8f).

9 Weathering

Weathering on planetary bodies produces regolith from rock via a range of breakdown processes, some of them unknown on Earth. The landscape expression of these weathering processes includes softening of primary landforms, such as impact craters, following a generally diffusive trend (Fassett et al., 2017; Soderblom, 1970). Landforms directly linked to weathering processes, include regolith surface textures and rock shapes, which tend to be expressed at the metre-scale or less. Hence, *in situ* observations are best suited to inferring weathering processes are limited to the Moon, Mars, asteroids Bennu and Ryugu and comet 67P.

On bodies without an atmosphere the surface is subject to a range of processes not experienced at Earth's surface, including solar wind sputtering and micrometeorite impacts. In addition, thermal stress and fatigue are greatly accentuated by the high amplitude thermal variations experienced on many planetary surfaces compared to Earth (El Mir et al., 2019; Molaro and Byrne, 2012). Cracked rocks or "Puzzle rocks" observed on Bennu (Walsh et al., 2019), Ryugu (Sasaki et al., 2021), the Moon (Ruesch et al., 2020) and Mars (Eppes et al., 2015; Hörz et al., 1999) have been linked to thermal fatigue and/or micrometeorite impacts (Figure 9a). On Mars rocks can also be sculpted by the wind – producing ventifacts (Bridges et al., 1999; Greeley et al., 2006a; Thomson et al., 2008) (see also Section 2). Pitted boulder surfaces on Mars have been linked to transient melting of snow (Head et al., 2011) and volatile-related processes have been implicated in accelerating rock chute formation (Levin et al., 2021) and boulder breakdown (de Haas et al., 2013).

A consequence of rock breakdown is rockfalls, which have been observed to occur in repeat imaging of Mars (Grindrod et al., 2021; Vijayan et al., 2021) (Figure 9b). Roll/bounce marks left in the regolith

in the wake of boulders (Figure 9c) have shown rockfall to be a recently active process on the Moon (Arvidson et al., 1975; Bickel et al., 2020). Patterns in the distribution of rockfall tracks have been used to provide evidence for rock breakdown by thermal stress on Mars on the timescale of < 1Ma (Tesson et al., 2020), seismic activity on Mars (Roberts et al., 2012) and on the Moon (Senthil Kumar et al., 2016), as well as inform the regolith strength on the Moon (Bickel and Kring, 2020).

Some puzzling aspects of surface regolith appearance have been attributed to surface sintering caused by solar irradiation (Zharkova et al., 2020) (Figure 9d).

10 Impact Cratering

The process of impact cratering dominates most planetary surfaces apart from the Earth, Venus, Titan and Io which either have dense atmospheres reducing the incoming impactor population and/or surface processes that act to erase any crater landforms that are created. Impact craters create topographic relief that can serve as a catalyst for other surface processes and they expose materials from planetary interiors to active surface processes. For example, impacts can cause substantial seismic shaking (Schultz and Gault, 1975) and therefore can initiate mass movements (see Section 7).

The shape of an impact crater is primarily a function of the gravity, impactor size and the target surface composition (Melosh, 1989). Other factors, such as impact speed and angle, impactor composition, or target structure, also play a role in modulating the crater shape, but for the purposes of this review will not be considered in further detail. With increasing impactor sizes craters evolve from “simple” bowl-shapes towards more “complex”, including flat-floored with a central peak up to multi-ringed basins (Figure 10a-c). The crater diameter at which the simple-to-complex transition occurs varies from planetary body to planetary body and is traditionally represented by plotting the population of craters on a logarithmic depth-diameter diagram. For example, on Mars the simple-to-complex transition occurs at crater diameters of ~8 km, on Europa it occurs at ~1 km and Vesta at 28 km (Hiesinger et al., 2016).

Impact craters eject material from their cavity forming unique morphologies, such as ejecta blankets, secondary crater clusters/chains, and visible radial “rays” which can be global in extent (Figure 10d). Impact melt, found within the cavity and in the ejecta, shares many morphological characteristics with lava and in ancient terrains on the Moon and Mercury, the distinction between them can be challenging (Denevi et al., 2013). The outcrops located in crater walls and central peaks can provide relatively fresh exposures of subsurface materials providing insights into the subsurface composition of a body without having to drill *in situ* (Quantin et al., 2012).

Impact craters substantially disturb the crust (Kenkmann et al., 2014) and as a result can form a structural conduit for endogenic processes that are then expressed at the surface, such as hydrothermal circulation (Osinski et al., 2013), explosive volcanism (Thomas et al., 2014), or cryovolcanism (Nathues et al., 2020).

Impact craters are used as an essential dating tool in planetary science, as their size-frequency distribution is a function of the exposure age of a surface (Hartmann and Neukum, 2001). The degradation state of the craters, hence the ability to recognise the surface processes that have influenced them, is an important factor when interpreting the results of the crater size-frequency distribution (Michael and Neukum, 2010).

11 Sublimation landforms and processes

Environments dominated by sublimation are rare on Earth, hence entire landforms or landscapes dominated by this phase change are restricted to other planetary bodies. In particular the icy satellites of the outer Solar System have surfaces dominated by various ices and whose sublimation is thought to explain some of the most unusual landscapes (Mangold, 2011). For example, the entire surface of Jupiter's moon Callisto is thought to have been extensively modified by the sublimation of CO_2 and H_2O ices at its surface leaving a terrain dominated by dissected ridges and knobs (Figure 11a) (White et al., 2016). Helene, in the Saturn system, has a sculpted surface attributed to remobilisation of a thick layer of particles whose origin is sublimation from the plumes of Enceladus (Figure 11b) (Hirata et al., 2014).

Comets are another planetary body where sublimation is the dominant landscape forming process every time the comet approaches the sun. The first cometary orbital data from the Rosetta mission to comet 67P revealed astonishingly diverse landscapes, including dunes (see Section 2), retreating steep sided pits and cliffs (Figure 11c) (Vincent et al., 2015) and cracks and fissures(El-Maarry et al., 2015). The steep sided pits and cliffs are thought to be correlated to the plumes of outgassing (Vincent et al., 2016). Gassy outbursts were also noted to mobilise dust on asteroid Bennu, yet the geomorphic effect if any in this setting remains unclear (Lauretta et al., 2019).

On other bodies, depressions are the most common landform associated with sublimation and can be considered akin to karst on Earth. The perennial CO_2 ice found at the South Polar cap of Mars, undergoes retreat each year in the form of enlarging and coalescing circular to elliptical steep sided pits typically several hundred metres in diameter and metres deep, dubbed "swiss cheese" (Buhler et al., 2017) (Figure 11d). The loss of excess water ice from the ground via sublimation in the mid-latitudes of Mars results in "scalloped depressions" (Dundas et al., 2015; Soare et al., 2007) – shallow-sloping depressions of hundreds of metres in extent, with an arcuate and steeper backwall. In the some of the same regions, sublimation expands polygonally patterned contraction cracks producing chains of pits and possibly cavities (Séjourné et al., 2011). Volatile loss has also been invoked to explain shallow, steep-sided depressions on Mercury which are surrounded by a relatively bright halo – "hollows" (Blewett et al., 2011) (Figure 11e). The discovery of these landforms was part of the realisation that Mercury's crust is not actually depleted in volatiles as once thought (Nittler and Weider, 2019).

The seasonal retreat of the CO_2 ice deposits across the surface of Mars results in a uniquely martian process caused by basal sublimation of the CO_2 ice (Kieffer et al., 2006). CO_2 ice is translucent to solar radiation, hence the increasing incoming solar radiation in late winter to early spring can heat the regolith under the CO_2 ice, causing it to sublimate and CO_2 gas to be trapped underneath it. The gas pressure builds until the ice above breaks, releasing the gas in a jet which deposits dark dust from under the ice onto the still bright icy surface. This phenomenon most commonly manifests itself as dark fans or spots (Hansen et al., 2013) and on the steep slopes of dunes can even appear as digitate (Gardin et al., 2010). The sediment mobilised under the ice is thought to explain the observation of "spiders" – dendritic networks of channels leading to one or more "nodes" (Thomas et al., 2011) (Figure 11f). Individual spiders can be hundreds of metres in size and they can extend across many kilometres. Although spiders have not been observed to grow, similar branching networks have been observed to appear and grow on dunes ("furrows") (Portyankina et al., 2010). Sediment mobilisation by sublimating CO_2 is thought to explain ongoing sediment motions observed in martian gullies which only occur in winter (Dundas et al., 2019). In particular, a uniquely martian morphology called "linear gullies" is thought to be formed by levitating blocks of CO_2 ice falling from icy dune crests (Diniega et

al., 2013). Volatile loss is believed to drive the formation of gully-like-landforms on the asteroid Vesta (Scully et al., 2015) and on Mercury (Malliband et al., 2019).

12 Discussion & Conclusions

Planetary geomorphology is distinctive from Earth-based geomorphology in that it is very reliant on remote sensing and often a more global-scale perspective is taken on unravelling the formation of landscapes and landforms. Satellite data of the Earth have spurred a number of studies taking a similar planetary-scale perspective on Earth (Chen et al., 2019; Poulos et al., 2012), but more often studies are local and/or regional in scale and scope. Planetary geomorphology is enticing to many, because of the aspect of exploration and the possibility of making unusual discoveries on alien worlds. Planetary geomorphology can drive key advances to better understand our own planet (Baker, 1993; Sharp, 1980).

One of the major limitations of planetary geomorphology is the problem of equifinality and the uncertainty of what landforms can be produced by processes unknown on Earth (Baker, 2014). To infer processes from landforms and landscapes is not an exact science and always open to interpretation. Access to the field can resolve many ambiguities on Earth, yet in a planetary context this is rarely an option and can lead to impasses where researchers just do not have enough data to disambiguate the leading hypotheses. Yet, as shown in this contribution, planetary geomorphology remains an essential tool in understanding the internal and external forces shaping bodies in the Solar System.

Planetary Geomorphology is likely to continue to grow, because the ability to interpret process from remote sensing data is key to planning future missions, for example deciding where to land or acquire certain types of data. Image and topographic data are the cornerstones of every new mission and future exploration will only add to our database of new and surprising planetary landforms and landscapes. Further, these landscapes have much to teach us about our own planet.

13 Acknowledgements

SJC is grateful to the CNES for financial support of her involvement in the ExoMars Trace Gas Orbiter CaSSIS, MRO HiRISE and BepiColombo missions. SJC received funding from the regional government Pays de la Loire scheme “Etoile Montantes” project METAFLOWS. The author thanks the spacecraft and instrument engineering teams for the successful completion and operation of CaSSIS. CaSSIS is a project of the University of Bern funded through the Swiss Space Office via ESA's PRODEX programme. The instrument hardware development was also supported by the Italian Space Agency (ASI) (ASI-INAF agreement no. I/018/12/0), INAF/ Astronomical Observatory of Padova, and the Space Research Center (CBK) in Warsaw. Support from SGF (Budapest), the University of Arizona (LPL) and NASA are also gratefully acknowledged. This study has been supported by the Italian Space Agency (ASI-INAF agreement no. 2020-17-HH.0).

14 References

Ahrens, C.J., 2020. Modeling cryogenic mud volcanism on Pluto. J. Volcanol. Geotherm. Res. 406, 107070. https://doi.org/10.1016/j.jvolgeores.2020.107070

Ansan, V., Mangold, N., Masson, P., Gailhardis, E., Neukum, G., 2008. Topography of valley networks on Mars from Mars Express High Resolution Stereo Camera digital elevation models. J. Geophys. Res. 113, E07006. https://doi.org/10.1029/2007JE002986

Arvidson, R., Drozd, R.J., Hohenberg, C.M., Morgan, C.J., Poupeau, G., 1975. Horizontal transport of the regolith, modification of features, and erosion rates on the lunar surface. The moon 13, 67–79. https://doi.org/10.1007/BF00567508

Baioni, D., Sgavetti, M., 2013. Karst terrains as possible lithologic and stratigraphic markers in northern Sinus Meridiani, Mars. Planet. Space Sci. 75, 173–181. https://doi.org/10.1016/j.pss.2012.08.011

Baker, V.R., 2014. Terrestrial analogs, planetary geology, and the nature of geological reasoning. Planet. Geol. Field Symp. Kitakyushu Jpn. 2011 Planet. Geol. Terr. Analogs 95, 5–10. https://doi.org/10.1016/j.pss.2012.10.008

Baker, V.R., 1993. Extraterrestrial geomorphology: science and philosophy of Earthlike planetary landscapes, in: Geomorphology: The Research Frontier and Beyond. Elsevier, pp. 9–35. https://doi.org/10.1016/B978-0-444-89971-2.50006-7

Baker, V.R., Kochel, R.C., 1979. Martian channel morphology: Maja and Kasei Valles. J. Geophys. Res. 84, 7961. https://doi.org/10.1029/JB084iB14p07961

Baker, V.R., Partridge, J.B., 1986. Small Martian valleys: Pristine and degraded morphology. J. Geophys. Res. Solid Earth 91, 3561–3572. https://doi.org/10.1029/JB091iB03p03561

Baker, V.R., Strom, R.G., Gulick, V.C., Kargel, J.S., Komatsu, G., Kale, V.S., 1991. Ancient oceans, ice sheets and the hydrological cycle on Mars. Nature 352, 589–594. https://doi.org/10.1038/352589a0

Balme, M., Greeley, R., 2006. Dust devils on Earth and Mars. Rev. Geophys. 44, RG3003. https://doi.org/10.1029/2005RG000188

Balme, M., Mangold, N., Baratoux, D., Costard, F., Gosselin, M., Masson, P., Pinet, P., Neukum, G., 2006. Orientation and distribution of recent gullies in the southern hemisphere of Mars: Observations from High Resolution Stereo Camera/Mars Express (HRSC/MEX) and Mars Orbiter Camera/Mars Global Surveyor (MOC/MGS) data. J. Geophys. Res. Planets 111, doi:10.1029/2005JE002607.

Balme, M.R., Pathare, A., Metzger, S.M., Towner, M.C., Lewis, S.R., Spiga, A., Fenton, L.K., Renno, N.O., Elliott, H.M., Saca, F.A., Michaels, T.I., Russell, P., Verdasca, J., 2012. Field measurements of horizontal forward motion velocities of terrestrial dust devils: Towards a proxy for ambient winds on Mars and Earth. Icarus 221, 632–645. https://doi.org/10.1016/j.icarus.2012.08.021

Basilevsky, A.T., Shalygin, E.V., Titov, D.V., Markiewicz, W.J., Scholten, F., Roatsch, Th., Kreslavsky, M.A., Moroz, L.V., Ignatiev, N.I., Fiethe, B., Osterloh, B., Michalik, H., 2012. Geologic interpretation of the near-infrared images of the surface taken by the Venus Monitoring Camera, Venus Express. Icarus 217, 434–450. https://doi.org/10.1016/j.icarus.2011.11.003

Beddingfield, C.B., Beyer, R.A., Singer, K.N., McKinnon, W.B., Runyon, K., Grundy, W., Stern, S.A., Bray, V., Dhingra, R., Moore, J.M., Ennico, K., Olkin, C.B., Schenk, P., Spencer, J.R., Weaver, H.A., Young, L.A., 2020. Landslides on Charon. Icarus 335, 113383. https://doi.org/10.1016/j.icarus.2019.07.017

Bernhardt, H., Reiss, D., Hiesinger, H., Ivanov, M.A., 2016. The honeycomb terrain on the Hellas basin floor, Mars: A case for salt or ice diapirism: Hellas' Honeycombs as Salt/Ice Diapirs. J. Geophys. Res. Planets 121, 714–738. https://doi.org/10.1002/2016JE005007

Bhardwaj, A., Sam, L., Martín-Torres, F.J., Zorzano, M.-P., Fonseca, R.M., 2017. Martian slope streaks as plausible indicators of transient water activity. Sci. Rep. 7. https://doi.org/10.1038/s41598-017-07453-9

Bickel, V.T., Aaron, J., Manconi, A., Loew, S., Mall, U., 2020. Impacts drive lunar rockfalls over billions of years. Nat. Commun. 11, 2862. https://doi.org/10.1038/s41467-020-16653-3

Bickel, V.T., Kring, D.A., 2020. Lunar south pole boulders and boulder tracks: Implications for crew and rover traverses. Icarus 348, 113850. https://doi.org/10.1016/j.icarus.2020.113850

Blewett, D.T., Chabot, N.L., Denevi, B.W., Ernst, C.M., Head, J.W., Izenberg, N.R., Murchie, S.L., Solomon, S.C., Nittler, L.R., McCoy, T.J., Xiao, Z., Baker, D.M.H., Fassett, C.I., Braden, S.E., Oberst, J., Scholten, F., Preusker, F., Hurwitz, D.M., 2011. Hollows on Mercury: MESSENGER

573 Evidence for Geologically Recent Volatile-Related Activity. Science 333, 1856–1859.
574 https://doi.org/10.1126/science.1211681
575 Bordiec, M., Carpy, S., Bourgeois, O., Herny, C., Massé, M., Perret, L., Claudin, P., Pochat, S., Douté,
576 S., 2020. Sublimation waves: Geomorphic markers of interactions between icy planetary
577 surfaces and winds. Earth-Sci. Rev. 211, 103350.
578 https://doi.org/10.1016/j.earscirev.2020.103350
579 Bourke, M.C., 2010. Barchan dune asymmetry: Observations from Mars and Earth. Icarus 205, 183–
580 197. https://doi.org/10.1016/j.icarus.2009.08.023
581 Bourke, M.C., Balme, M., Lewis, S., Lorenz, R.D., Parteli, E., 2019. Planetary Aeolian Geomorphology.
582 Aeolian Geomorphol. New Introd. 261–286.
583 Boyce, J.M., Mouginis-Mark, P., Robinson, M., 2020. The Tsiolkovskiy crater landslide, the moon: An
584 LROC view. Icarus 337, 113464. https://doi.org/10.1016/j.icarus.2019.113464
585 Bridges, N.T., Greeley, R., Haldemann, A.F.C., Herkenhoff, K.E., Kraft, M., Parker, T.J., Ward, A.W.,
586 1999. Ventifacts at the Pathfinder landing site. J. Geophys. Res. Planets 104, 8595–8615.
587 https://doi.org/10.1029/98JE02550
588 Brož, P., Hauber, E., 2012. A unique volcanic field in Tharsis, Mars: Pyroclastic cones as evidence for
589 explosive eruptions. Icarus 218, 88–99. https://doi.org/10.1016/j.icarus.2011.11.030
590 Brož, P., Krýza, O., Wilson, L., Conway, S.J., Hauber, E., Mazzini, A., Raack, J., Balme, M.R., Sylvest,
591 M.E., Patel, M.R., 2020. Experimental evidence for lava-like mud flows under Martian surface
592 conditions. Nat. Geosci. 13, 403–407. https://doi.org/10.1038/s41561-020-0577-2
593 Brunetti, M.T., Xiao, Z., Komatsu, G., Peruccacci, S., Guzzetti, F., 2015. Large rock slides in impact
594 craters on the Moon and Mercury. Icarus 260, 289–300.
595 https://doi.org/10.1016/j.icarus.2015.07.014
596 Brusnikin, E.S., Kreslavsky, M.A., Zubarev, A.E., Patratiy, V.D., Krasilnikov, S.S., Head, J.W.,
597 Karachevtseva, I.P., 2016. Topographic measurements of slope streaks on Mars. Icarus 278,
598 52–61. https://doi.org/10.1016/j.icarus.2016.06.005
599 Buhler, P.B., Ingersoll, A.P., Ehlmann, B.L., Fassett, C.I., Head, J.W., 2017. How the martian residual
600 south polar cap develops quasi-circular and heart-shaped pits, troughs, and moats. Icarus
601 286, 69–93. https://doi.org/10.1016/j.icarus.2017.01.012
602 Buldovicz, S.N., Khilimonyuk, V.Z., Bychkov, A.Y., Ospennikov, E.N., Vorobyev, S.A., Gunar, A.Y.,
603 Gorshkov, E.I., Chuvilin, E.M., Cherbunina, M.Y., Kotov, P.I., Lubnina, N.V., Motenko, R.G.,
604 Amanzhurov, R.M., 2018. Cryovolcanism on the Earth: Origin of a Spectacular Crater in the
605 Yamal Peninsula (Russia). Sci. Rep. 8, 13534. https://doi.org/10.1038/s41598-018-31858-9
606 Burns, J.A., 2010. The four hundred years of planetary science since Galileo and Kepler. Nature 466,
607 575–584. https://doi.org/10.1038/nature09215
608 Burr, D.M., Tanaka, K.L., Yoshikawa, K., 2009. Pingos on Earth and Mars. Planet. Space Sci. 57, 541–
609 555. https://doi.org/10.1016/j.pss.2008.11.003
610 Butcher, F.E.G., Balme, M.R., Conway, S.J., Gallagher, C.J., Arnold, N.S., Storrar, R.D., Lewis, S.R.,
611 Hagermann, A., 2020. Morphometry of a Glacier-Linked Esker in NW Tempe Terra, Mars, and
612 Implications for Sediment-Discharge Dynamics of Subglacial Drainage. Earth Planet. Sci. Lett.
613 542, 116325. https://doi.org/10.1016/j.epsl.2020.116325
614 Butcher, F.E.G., Conway, S.J., Arnold, N.S., 2016. Are the Dorsa Argentea on Mars eskers? Icarus 275,
615 65–84. https://doi.org/10.1016/j.icarus.2016.03.028
616 Byrne, P.K., Ghail, R.C., Şengör, A.M.C., James, P.B., Klimczak, C., Solomon, S.C., 2021. A globally
617 fragmented and mobile lithosphere on Venus. Proc. Natl. Acad. Sci. 118, e2025919118.
618 https://doi.org/10.1073/pnas.2025919118
619 Byrne, P.K., Klimczak, C., Celâl Şengör, A.M., Solomon, S.C., Watters, T.R., Hauck, II, S.A., 2014.
620 Mercury's global contraction much greater than earlier estimates. Nat. Geosci. 7, 301–307.
621 https://doi.org/10.1038/ngeo2097
622 Byrne, P.K., Klimczak, C., Williams, D.A., Hurwitz, D.M., Solomon, S.C., Head, J.W., Preusker, F.,
623 Oberst, J., 2013. An assemblage of lava flow features on Mercury: LAVA FLOW FEATURES ON
624 MERCURY. J. Geophys. Res. Planets 118, 1303–1322. https://doi.org/10.1002/jgre.20052

625 Cabrol, N., Grin, E.A., 1999. Distribution, Classification, and Ages of Martian Impact Crater Lakes.
626 Icarus 142, 160–172. https://doi.org/10.1006/icar.1999.6191
627 Carr, M., Head, J., 2019. Mars: Formation and fate of a frozen Hesperian ocean. Icarus 319, 433–443.
628 https://doi.org/10.1016/j.icarus.2018.08.021
629 Chen, S.-A., Michaelides, K., Grieve, S.W.D., Singer, M.B., 2019. Aridity is expressed in river
630 topography globally. Nature 573, 573–577. https://doi.org/10.1038/s41586-019-1558-8
631 Chuang, F.C., Beyer, R.A., McEwen, A.S., Thomson, B.J., 2007. HiRISE observations of slope streaks on
632 Mars. Geophys. Res. Lett. 34, doi:10.1029/2007GL031111. https://doi.org/L20204 Artn
633 l20204
634 Citron, R.I., Manga, M., Hemingway, D.J., 2018. Timing of oceans on Mars from shoreline
635 deformation. Nature 555, 643–646. https://doi.org/10.1038/nature26144
636 Collins, G.C., McKinnon, W.B., Moore, J.M., Nimmo, F., Pappalardo, R.T., Prockter, L.M., Schenk, P.M.,
637 2009. Tectonics of the outer planet satellites. Planet. Tecton. 11, 229.
638 Conway, S.J., Balme, M.R., 2016. A novel topographic parameterization scheme indicates that
639 martian gullies display the signature of liquid water. Earth Planet. Sci. Lett. 454, 36–45.
640 https://doi.org/10.1016/j.epsl.2016.08.031
641 Conway, S.J., de Haas, T., Harrison, T.N., 2019. Martian gullies: a comprehensive review of
642 observations, mechanisms and the insights from Earth analogues. Geol. Soc. Lond. Spec.
643 Publ. 467. https://doi.org/10.1144/SP467.14
644 Costard, F., Sejourne, A., Kargel, J., Godin, E., 2016. Modeling and observational occurrences of near-
645 surface drainage in Utopia Planitia, Mars. Geomorphology 275, 80–89.
646 https://doi.org/10.1016/j.geomorph.2016.09.034
647 Costard, F., Séjourné, A., Kelfoun, K., Clifford, S., Lavigne, F., Di Pietro, I., Bouley, S., 2017. Modeling
648 tsunami propagation and the emplacement of thumbprint terrain in an early Mars ocean:
649 TSUNAMIS ON MARS. J. Geophys. Res. Planets 122, 633–649.
650 https://doi.org/10.1002/2016JE005230
651 Crane, K., 2020. Structural interpretation of thrust fault-related landforms on Mercury using Earth
652 analogue fault models. Geomorphology 369, 107366.
653 https://doi.org/10.1016/j.geomorph.2020.107366
654 Crosta, G.B., Frattini, P., Valbuzzi, E., De Blasio, F.V., 2018. Introducing a New Inventory of Large
655 Martian Landslides. Earth Space Sci. 5, 89–119. https://doi.org/10.1002/2017EA000324
656 Davis, J.M., Balme, M., Grindrod, P.M., Williams, R.M.E., Gupta, S., 2016. Extensive Noachian fluvial
657 systems in Arabia Terra: Implications for early Martian climate. Geology 44, 847–850.
658 https://doi.org/10.1130/G38247.1
659 Day, M., Kocurek, G., 2016. Observations of an aeolian landscape: From surface to orbit in Gale
660 Crater. Icarus 280, 37–71. https://doi.org/10.1016/j.icarus.2015.09.042
661 de Haas, T., Hauber, E., Conway, S.J., van Steijn, H., Johnsson, A., Kleinhans, M.G., 2015. Earth-like
662 aqueous debris-flow activity on Mars at high orbital obliquity in the last million years. Nat.
663 Commun. 6. https://doi.org/10.1038/ncomms8543
664 de Haas, T., Hauber, E., Kleinhans, M.G., 2013. Local late Amazonian boulder breakdown and
665 denudation rate on Mars. Geophys. Res. Lett. https://doi.org/10.1002/grl.50726
666 Dehouck, E., Mangold, N., Le Mouélic, S., Ansan, V., Poulet, F., 2010. Ismenius Cavus, Mars: A deep
667 paleolake with phyllosilicate deposits. Planet. Space Sci. 58, 941–946.
668 https://doi.org/10.1016/j.pss.2010.02.005
669 Denevi, B.W., Ernst, C.M., Meyer, H.M., Robinson, M.S., Murchie, S.L., Whitten, J.L., Head, J.W.,
670 Watters, T.R., Solomon, S.C., Ostrach, L.R., Chapman, C.R., Byrne, P.K., Klimczak, C.,
671 Peplowski, P.N., 2013. The distribution and origin of smooth plains on Mercury: SMOOTH
672 PLAINS ON MERCURY. J. Geophys. Res. Planets 118, 891–907.
673 https://doi.org/10.1002/jgre.20075
674 Di Achille, G., Hynek, B.M., 2010. Ancient ocean on Mars supported by global distribution of deltas
675 and valleys. Nat. Geosci. 3, 459–463. https://doi.org/10.1038/ngeo891

Diniega, S., Byrne, S., Bridges, N.T., Dundas, C.M., McEwen, A.S., 2010. Seasonality of present-day Martian dune-gully activity. Geology 38, 1047–1050. https://doi.org/10.1130/G31287.1

Diniega, S., Hansen, C.J., McElwaine, J.N., Hugenholtz, C.H., Dundas, C.M., McEwen, A.S., Bourke, M.C., 2013. A new dry hypothesis for the formation of martian linear gullies. Icarus 225, 526–537. https://doi.org/10.1016/j.icarus.2013.04.006

Duarte, K.D., Schmidt, B.E., Chilton, H.T., Hughson, K.H.G., Sizemore, H.G., Ferrier, K.L., Buffo, J.J., Scully, J.E.C., Nathues, A., Platz, T., Landis, M., Byrne, S., Bland, M., Russell, C.T., Raymond, C.A., 2019. Landslides on Ceres: Diversity and Geologic Context. J. Geophys. Res. Planets 2018JE005673. https://doi.org/10.1029/2018JE005673

Dundas, C.M., 2020. Geomorphological evidence for a dry dust avalanche origin of slope streaks on Mars. Nat. Geosci. 13, 473–476. https://doi.org/10.1038/s41561-020-0598-x

Dundas, C.M., Byrne, S., McEwen, A.S., 2015. Modeling the development of martian sublimation thermokarst landforms. Icarus 262, 154–169. https://doi.org/10.1016/j.icarus.2015.07.033

Dundas, C.M., McEwen, A.S., Diniega, S., Hansen, C.J., Byrne, S., McElwaine, J.N., 2019. The Formation of Gullies on Mars Today. Geol. Soc. Lond. Spec. Publ. Martian Gullies and their Earth Analogues. https://doi.org/10.1144/SP467.5

El Mir, C., Ramesh, K.T., Delbo, M., 2019. The efficiency of thermal fatigue in regolith generation on small airless bodies. Icarus 333, 356–370. https://doi.org/10.1016/j.icarus.2019.06.001

El-Maarry, M.R., Thomas, N., Gracia-Berná, A., Marschall, R., Auger, A.-T., Groussin, O., Mottola, S., Pajola, M., Massironi, M., Marchi, S., Höfner, S., Preusker, F., Scholten, F., Jorda, L., Kührt, E., Keller, H.U., Sierks, H., A'Hearn, M.F., Barbieri, C., Barucci, M.A., Bertaux, J.-L., Bertini, I., Cremonese, G., Da Deppo, V., Davidsson, B., Debei, S., De Cecco, M., Deller, J., Güttler, C., Fornasier, S., Fulle, M., Gutierrez, P.J., Hofmann, M., Hviid, S.F., Ip, W.-H., Knollenberg, J., Koschny, D., Kovacs, G., Kramm, J.-R., Küppers, M., Lamy, P.L., Lara, L.M., Lazzarin, M., Lopez Moreno, J.J., Marzari, F., Michalik, H., Naletto, G., Oklay, N., Pommerol, A., Rickman, H., Rodrigo, R., Tubiana, C., Vincent, J.-B., 2015. Fractures on comet 67P/Churyumov-Gerasimenko observed by Rosetta/OSIRIS: FRACTURES ON COMET 67P. Geophys. Res. Lett. 42, 5170–5178. https://doi.org/10.1002/2015GL064500

Eppes, M.-C., Willis, A., Molaro, J., Abernathy, S., Zhou, B., 2015. Cracks in Martian boulders exhibit preferred orientations that point to solar-induced thermal stress. Nat. Commun. 6, 6712. https://doi.org/10.1038/ncomms7712

Ewing, R.C., Lapotre, M.G.A., Lewis, K.W., Day, M., Stein, N., Rubin, D.M., Sullivan, R., Banham, S., Lamb, M.P., Bridges, N.T., Gupta, S., Fischer, W.W., 2017. "Sedimentary processes of the Bagnold Dunes: Implications for the eolian rock record of Mars": Bagnold Dune Field sedimentary processes. J. Geophys. Res. Planets. https://doi.org/10.1002/2017JE005324

Fassett, C.I., Crowley, M.C., Leight, C., Dyar, M.D., Minton, D.A., Hirabayashi, M., Thomson, B.J., Watters, W.A., 2017. Evidence for rapid topographic evolution and crater degradation on Mercury from simple crater morphometry: Rapid Crater Degradation on Mercury. Geophys. Res. Lett. https://doi.org/10.1002/2017GL073769

Fassett, C.I., Head III, J.W., 2008. The timing of martian valley network activity: Constraints from buffered crater counting. Icarus 195, 61–89. https://doi.org/10.1016/j.icarus.2007.12.009

Fastook, J.L., Head, J.W., 2015. Glaciation in the Late Noachian Icy Highlands: Ice accumulation, distribution, flow rates, basal melting, and top-down melting rates and patterns. Planet. Space Sci. 106, 82–98. https://doi.org/10.1016/j.pss.2014.11.028

Feldman, W.C., Pathare, A., Maurice, S., Prettyman, T.H., Lawrence, D.J., Milliken, R.E., Travis, B.J., 2011. Mars Odyssey neutron data: 2. Search for buried excess water ice deposits at nonpolar latitudes on Mars. J Geophys Res 116, E11009. https://doi.org/10.1029/2011JE003806

Ferri, F., Smith, P.H., Lemmon, M., Rennó, N.O., 2003. Dust devils as observed by Mars Pathfinder: DUST DEVILS AS OBSERVED BY MARS PATHFINDER. J. Geophys. Res. Planets 108. https://doi.org/10.1029/2000JE001421

Ferrill, D.A., Wyrick, D.Y., Smart, K.J., 2011. Coseismic, dilational-fault and extension-fracture related pit chain formation in Iceland: Analog for pit chains on Mars. Lithosphere 3, 133–142. https://doi.org/10.1130/L123.1

Gallagher, C., Balme, M., 2015. Eskers in a complete, wet-based glacial system in the Phlegra Montes region, Mars. Earth Planet. Sci. Lett. 431, 96–109. https://doi.org/10.1016/j.epsl.2015.09.023

Gallagher, C., Balme, M.R., Conway, S.J., Grindrod, P.M., 2011. Sorted clastic stripes, lobes and associated gullies in high-latitude craters on Mars: Landforms indicative of very recent, polycyclic ground-ice thaw and liquid flows. Icarus 211, 458–471. https://doi.org/10.1016/j.icarus.2010.09.010

Gardin, E., Allemand, P., Quantin, C., Thollot, P., 2010. Defrosting, dark flow features, and dune activity on Mars: Example in Russell crater. J Geophys Res 115, doi:10.1029/2009JE003515. https://doi.org/10.1029/2009je003515

Gastineau, R., Conway, S.J., Johnsson, A., Eichel, J., Mangold, N., Grindrod, P.M., Izquierdo, T., 2020. Small-scale lobate hillslope features on Mars: A comparative 3D morphological study with terrestrial solifluction lobes and zebra stripe lobes. Icarus accepted.

Ghatan, G., Zimbelman, J., 2006. Paucity of candidate coastal constructional landforms along proposed shorelines on Mars: Implications for a northern lowlands-filling ocean. Icarus 185, 171–196. https://doi.org/10.1016/j.icarus.2006.06.007

Goudge, T.A., Aureli, K.L., Head, J.W., Fassett, C.I., Mustard, J.F., 2015. Classification and analysis of candidate impact crater-hosted closed-basin lakes on Mars. Icarus 260, 346–367. https://doi.org/10.1016/j.icarus.2015.07.026

Goudge, T.A., Fassett, C.I., Head, J.W., Mustard, J.F., Aureli, K.L., 2016. Insights into surface runoff on early Mars from paleolake basin morphology and stratigraphy. Geology 44, 419–422. https://doi.org/10.1130/G37734.1

Goudie, A.S., 2007. Mega-Yardangs: A Global Analysis: Mega-yardangs: A global analysis. Geogr. Compass 1, 65–81. https://doi.org/10.1111/j.1749-8198.2006.00003.x

Grau Galofre, A., Jellinek, A.M., Osinski, G.R., 2020. Valley formation on early Mars by subglacial and fluvial erosion. Nat. Geosci. https://doi.org/10.1038/s41561-020-0618-x

Greeley, R., Arvidson, R.E., Barlett, P.W., Blaney, D., Cabrol, N.A., Christensen, P.R., Fergason, R.L., Golombek, M.P., Landis, G.A., Lemmon, M.T., McLennan, S.M., Maki, J.N., Michaels, T., Moersch, J.E., Neakrase, L.D.V., Rafkin, S.C.R., Richter, L., Squyres, S.W., de Souza, P.A., Sullivan, R.J., Thompson, S.D., Whelley, P.L., 2006a. Gusev crater: Wind-related features and processes observed by the Mars Exploration Rover Spirit: GUSEV CRATER OBSERVED BY SPIRIT. J. Geophys. Res. Planets 111, n/a-n/a. https://doi.org/10.1029/2005JE002491

Greeley, R., Bender, K., Thomas, P.E., Schubert, G., Limonadi, D., Weitz, C.M., 1995. Wind-Related Features and Processes on Venus: Summary of Magellan Results. Icarus 115, 399–420. https://doi.org/10.1006/icar.1995.1107

Greeley, R., Whelley, P.L., Arvidson, R.E., Cabrol, N.A., Foley, D.J., Franklin, B.J., Geissler, P.G., Golombek, M.P., Kuzmin, R.O., Landis, G.A., Lemmon, M.T., Neakrase, L.D.V., Squyres, S.W., Thompson, S.D., 2006b. Active dust devils in Gusev crater, Mars: Observations from the Mars Exploration Rover Spirit: ACTIVE DUST DEVILS IN GUSEV CRATER, MARS. J. Geophys. Res. Planets 111, n/a-n/a. https://doi.org/10.1029/2006JE002743

Grindrod, P.M., Balme, M.R., 2010. Groundwater processes in Hebes Chasma, Mars: GROUNDWATER AND HYDRATES ON MARS. Geophys. Res. Lett. 37, n/a-n/a. https://doi.org/10.1029/2010GL044122

Grindrod, P.M., Davis, J.M., Conway, S.J., de Haas, T., 2021. Active Boulder Falls in Terra Sirenum, Mars: Constraints on Timing and Causes. Geophys. Res. Lett. Accepted.

Gustafson, J.O., Bell, J.F., Gaddis, L.R., Hawke, B.R., Giguere, T.A., 2012. Characterization of previously unidentified lunar pyroclastic deposits using Lunar Reconnaissance Orbiter Camera data: NEW PYROCLASTIC DEPOSITS. J. Geophys. Res. Planets 117, n/a-n/a. https://doi.org/10.1029/2011JE003893

Hansen, C.J., Byrne, S., Portyankina, G., Bourke, M., Dundas, C., McEwen, A., Mellon, M., Pommerol, A., Thomas, N., 2013. Observations of the northern seasonal polar cap on Mars: I. Spring sublimation activity and processes. Mars Polar Sci. V 225, 881–897. https://doi.org/10.1016/j.icarus.2012.09.024

Hargitai, H., Kereszturi, Á. (Eds.), 2015. Encyclopedia of Planetary Landforms, Springer reference. Springer, New York.

Harrison, K.P., Grimm, R.E., 2003. Rheological constraints on martian landslides. Icarus 163, 347–362. https://doi.org/10.1016/S0019-1035(03)00045-9

Harrison, T.N., Osinski, G.R., Tornabene, L.L., Jones, E., 2015. Global Documentation of Gullies with the Mars Reconnaissance Orbiter Context Camera and Implications for Their Formation. Icarus 252, 236–254. https://doi.org/10.1016/j.icarus.2015.01.022

Hartmann, W.K., Neukum, G., 2001. Cratering Chronology and the Evolution of Mars. Space Sci. Rev. 96, 165–194. https://doi.org/10.1023/A:1011945222010

Head, J.W., Crumpler, L.S., Aubele, J.C., Guest, J.E., Saunders, R.S., 1992. Venus volcanism: Classification of volcanic features and structures, associations, and global distribution from Magellan data. J. Geophys. Res. 97, 13153. https://doi.org/10.1029/92JE01273

Head, J.W., Kreslavsky, M.A., Marchant, D.R., 2011. Pitted rock surfaces on Mars: A mechanism of formation by transient melting of snow and ice. J. Geophys. Res. 116, E09007. https://doi.org/10.1029/2011JE003826

Head, J.W., Marchant, D.R., 2003. Cold-based mountain glaciers on Mars: Western Arsia Mons. Geology 31, 641–644. https://doi.org/10.1130/0091-7613(2003)031<0641:CMGOMW>2.0.CO;2

Herrero-Gil, A., Egea-González, I., Ruiz, J., Romeo, I., 2019. Structural modeling of lobate scarps in the NW margin of Argyre impact basin, Mars. Icarus 319, 367–380. https://doi.org/10.1016/j.icarus.2018.09.027

Hiesinger, H., Marchi, S., Schmedemann, N., Schenk, P., Pasckert, J.H., Neesemann, A., O'Brien, D.P., Kneissl, T., Ermakov, A.I., Fu, R.R., Bland, M.T., Nathues, A., Platz, T., Williams, D.A., Jaumann, R., Castillo-Rogez, J.C., Ruesch, O., Schmidt, B., Park, R.S., Preusker, F., Buczkowski, D.L., Russell, C.T., Raymond, C.A., 2016. Cratering on Ceres: Implications for its crust and evolution. Science 353, aaf4759. https://doi.org/10.1126/science.aaf4759

Hirata, N., Miyamoto, H., Showman, A.P., 2014. Particle deposition on the saturnian satellites from ephemeral cryovolcanism on Enceladus. Geophys. Res. Lett. 41, 4135–4141. https://doi.org/10.1002/2014GL060470

Hörz, F., Cintala, M.J., Rochelle, W.C., Kirk, B., 1999. Collisionally Processed Rocks on Mars. Science 285, 2105–2107. https://doi.org/10.1126/science.285.5436.2105

Howard, A.D., Moore, J.M., Umurhan, O.M., White, O.L., Anderson, R.S., McKinnon, W.B., Spencer, J.R., Schenk, P.M., Beyer, R.A., Stern, S.A., Ennico, K., Olkin, C.B., Weaver, H.A., Young, L.A., 2017a. Present and past glaciation on Pluto. Spec. Issue Pluto Syst. 287, 287–300. https://doi.org/10.1016/j.icarus.2016.07.006

Howard, A.D., Moore, J.M., White, O.L., Umurhan, O.M., Schenk, P.M., Grundy, W.M., Schmitt, B., Philippe, S., McKinnon, W.B., Spencer, J.R., Beyer, R.A., Stern, S.A., Ennico, K., Olkin, C.B., Weaver, H.A., Young, L.A., 2017b. Pluto: Pits and mantles on uplands north and east of Sputnik Planitia. Icarus 293, 218–230. https://doi.org/10.1016/j.icarus.2017.02.027

Hurwitz, D.M., Head, J.W., Hiesinger, H., 2013. Lunar sinuous rilles: Distribution, characteristics, and implications for their origin. Planet. Space Sci. 79–80, 1–38. https://doi.org/10.1016/j.pss.2012.10.019

Ielpi, A., Lapôtre, M.G.A., 2020. A tenfold slowdown in river meander migration driven by plant life. Nat. Geosci. 13, 82–86. https://doi.org/10.1038/s41561-019-0491-7

Jia, P., Andreotti, B., Claudin, P., 2017. Giant ripples on comet 67P/Churyumov–Gerasimenko sculpted by sunset thermal wind. Proc. Natl. Acad. Sci. 114, 2509–2514. https://doi.org/10.1073/pnas.1612176114

828 Johnson, B.C., Campbell, C.S., 2017. Drop Height and Volume Control the Mobility of Long-Runout
829 Landslides on the Earth and Mars: The Mobility of Long-Runout Landslides on the Earth and
830 Mars. Geophys. Res. Lett. https://doi.org/10.1002/2017GL076113
831 Johnson, B.C., Sori, M.M., 2020. Landslide Morphology and Mobility on Ceres Controlled by
832 Topography. J. Geophys. Res. Planets 125. https://doi.org/10.1029/2020JE006640
833 Johnsson, A., Reiss, D., Hauber, E., Zanetti, M., Hiesinger, H., Johansson, L., Olvmo, M., 2012.
834 Periglacial mass-wasting landforms on Mars suggestive of transient liquid water in the recent
835 past: Insights from solifluction lobes on Svalbard. Icarus 218, 489–505.
836 https://doi.org/10.1016/j.icarus.2011.12.021
837 Jones, A.P., Pickering, K.T., 2003. Evidence for aqueous fluid–sediment transport and erosional
838 processes on Venus. J. Geol. Soc. 160, 319–327. https://doi.org/10.1144/0016-764902-111
839 Kargel, J.S., 1995. Cryovolcanism on the Icy Satellites, in: Chahine, M.T., A'Hearn, M.F., Rahe, J.,
840 Solomon, P., Nickle, N.L. (Eds.), Comparative Planetology with an Earth Perspective. Springer
841 Netherlands, Dordrecht, pp. 101–113. https://doi.org/10.1007/978-94-017-1092-3_12
842 Kargel, J.S., Kirk, R.L., Fegley, B., Treiman, A.H., 1994. Carbonate-Sulfate Volcanism on Venus? Icarus
843 112, 219–252. https://doi.org/10.1006/icar.1994.1179
844 Karlsson, N.B., Schmidt, L.S., Hvidberg, C.S., 2015. Volume of Martian midlatitude glaciers from radar
845 observations and ice flow modeling. Geophys. Res. Lett. 42, 2627–2633.
846 https://doi.org/10.1002/2015GL063219
847 Kattenhorn, S.A., Prockter, L.M., 2014. Evidence for subduction in the ice shell of Europa. Nat. Geosci.
848 7, 762–767. https://doi.org/10.1038/ngeo2245
849 Kenkmann, T., Poelchau, M.H., Wulf, G., 2014. Structural geology of impact craters. J. Struct. Geol.
850 62, 156–182. https://doi.org/10.1016/j.jsg.2014.01.015
851 Kerber, L., Head, J.W., Blewett, D.T., Solomon, S.C., Wilson, L., Murchie, S.L., Robinson, M.S., Denevi,
852 B.W., Domingue, D.L., 2011. The global distribution of pyroclastic deposits on Mercury: The
853 view from MESSENGER flybys 1–3. Planet. Space Sci. 59, 1895–1909.
854 https://doi.org/10.1016/j.pss.2011.03.020
855 Kieffer, H.H., 1990. H2O grain size and the amount of dust in Mars' residual north polar CAP. J.
856 Geophys. Res. 95, 1481–1493.
857 Kieffer, H.H., Christensen, P.R., Titus, T.N., 2006. CO2 jets formed by sublimation beneath translucent
858 slab ice in Mars' seasonal south polar ice cap. Nature 442, 793–796.
859 https://doi.org/10.1038/nature04945
860 Knight, J., 2008. The environmental significance of ventifacts: A critical review. Earth-Sci. Rev. 86, 89–
861 105. https://doi.org/10.1016/j.earscirev.2007.08.003
862 Kok, J.F., Parteli, E.J.R., Michaels, T.I., Karam, D.B., 2012. The physics of wind-blown sand and dust.
863 Rep. Prog. Phys. 75, 106901. https://doi.org/10.1088/0034-4885/75/10/106901
864 Komatsu, G., Baker, V.R., 1994. Meander properties of Venusian channels. Geology 22, 67.
865 https://doi.org/10.1130/0091-7613(1994)022<0067:MPOVC>2.3.CO;2
866 Laity, J.E., Bridges, N.T., 2009. Ventifacts on Earth and Mars: Analytical, field, and laboratory studies
867 supporting sand abrasion and windward feature development. Geomorphology 105, 202–
868 217. https://doi.org/10.1016/j.geomorph.2008.09.014
869 Lapotre, M.G.A., Lamb, M.P., 2018. Substrate controls on valley formation by groundwater on Earth
870 and Mars. Geology 46, 531–534. https://doi.org/10.1130/G40007.1
871 Lapôtre, M.G.A., O'Rourke, J.G., Schaefer, L.K., Siebach, K.L., Spalding, C., Tikoo, S.M., Wordsworth,
872 R.D., 2020. Probing space to understand Earth. Nat. Rev. Earth Environ. 1, 170–181.
873 https://doi.org/10.1038/s43017-020-0029-y
874 Lauretta, D.S., Hergenrother, C.W., Chesley, S.R., Leonard, J.M., Pelgrift, J.Y., Adam, C.D., Al Asad, M.,
875 Antreasian, P.G., Ballouz, R.-L., Becker, K.J., Bennett, C.A., Bos, B.J., Bottke, W.F., Brozović,
876 M., Campins, H., Connolly, H.C., Daly, M.G., Davis, A.B., de León, J., DellaGiustina, D.N.,
877 Drouet d'Aubigny, C.Y., Dworkin, J.P., Emery, J.P., Farnocchia, D., Glavin, D.P., Golish, D.R.,
878 Hartzell, C.M., Jacobson, R.A., Jawin, E.R., Jenniskens, P., Kidd, J.N., Lessac-Chenen, E.J., Li, J.-
879 Y., Libourel, G., Licandro, J., Liounis, A.J., Maleszewski, C.K., Manzoni, C., May, B., McCarthy,

L.K., McMahon, J.W., Michel, P., Molaro, J.L., Moreau, M.C., Nelson, D.S., Owen, W.M., Rizk, B., Roper, H.L., Rozitis, B., Sahr, E.M., Scheeres, D.J., Seabrook, J.A., Selznick, S.H., Takahashi, Y., Thuillet, F., Tricarico, P., Vokrouhlický, D., Wolner, C.W.V., 2019. Episodes of particle ejection from the surface of the active asteroid (101955) Bennu. Science 366, eaay3544. https://doi.org/10.1126/science.aay3544

Leverington, D.W., 2011. A volcanic origin for the outflow channels of Mars: Key evidence and major implications. Geomorphology 132, 51–75. https://doi.org/10.1016/j.geomorph.2011.05.022

Levin, J.N., Dickson, J.L., Lamb, M.P., 2021. Evaluating the Role of Volatiles in Bedrock Chute Formation on the Moon and Mars. Icarus In review.

Lorenz, R., Zimbelman, J.R., 2014. Dune worlds: how windblown sand shapes planetary landscapes, Springer Praxis books. Geophysical sciences. Springer ; Published in association with Praxis Publishing, Berlin ; New York ; London : Chichester, UK.

Lucchetti, A., Penasa, L., Pajola, M., Massironi, M., Brunetti, M.T., Cremonese, G., Oklay, N., Vincent, J., Mottola, S., Fornasier, S., Sierks, H., Naletto, G., Lamy, P.L., Rodrigo, R., Koschny, D., Davidsson, B., Barbieri, C., Barucci, M.A., Bertaux, J., Bertini, I., Bodewits, D., Cambianica, P., Da Deppo, V., Debei, S., De Cecco, M., Deller, J., Ferrari, S., Ferri, F., Franceschi, M., Fulle, M., Gutiérrez, P., Güttler, C., Ip, W., Keller, U., Lara, L., Lazzarin, M., Moreno, J.L., Marzari, F., Tubiana, C., 2019. The Rocky-Like Behavior of Cometary Landslides on 67P/Churyumov-Gerasimenko. Geophys. Res. Lett. 46, 14336–14346. https://doi.org/10.1029/2019GL085132

Luo, W., Howard, A.D., 2008. Computer simulation of the role of groundwater seepage in forming Martian valley networks. J. Geophys. Res. Planets 113, E05002. https://doi.org/10.1029/2007JE002981

MacKenzie, S.M., Barnes, J.W., Sotin, C., Soderblom, J.M., Le Mouélic, S., Rodriguez, S., Baines, K.H., Buratti, B.J., Clark, R.N., Nicholson, P.D., McCord, T.B., 2014. Evidence of Titan's climate history from evaporite distribution. Icarus 243, 191–207. https://doi.org/10.1016/j.icarus.2014.08.022

Madeleine, J.-B., Forget, F., Millour, E., Montabone, L., Wolff, M.J., 2011. Revisiting the radiative impact of dust on Mars using the LMD Global Climate Model. J. Geophys. Res. 116, E11010. https://doi.org/10.1029/2011JE003855

Malin, M.C., Edgett, K.S., 2000. Evidence for recent groundwater seepage and surface runoff on Mars. Science 288, 2330–2335. https://doi.org/10.1126/science.288.5475.2330

Malin, M.C., Edgett, K.S., 1999. Oceans or seas in the Martian northern lowlands: High resolution imaging tests of proposed coastlines. Geophys. Res. Lett. 26, 3049–3052. https://doi.org/10.1029/1999GL002342

Malliband, C.C., Conway, S.J., Rothery, D.A., Balme, M.R., 2019. Potential Identification of Downslope Mass Movements on Mercury Driven by Volatile-Loss, in: Lunar and Planetary Science Conference. p. #1804.

Mangold, N., 2012. Fluvial landforms on fresh impact ejecta on Mars. Planet. Space Sci. 62, 69–85. https://doi.org/10.1016/j.pss.2011.12.009

Mangold, N., 2011. Ice sublimation as a geomorphic process: A planetary perspective. Geomorphology 126, 1–17. https://doi.org/10.1016/j.geomorph.2010.11.009

Mangold, N., 2005. High latitude patterned grounds on Mars: Classification, distribution and climatic control. Mars Polar Sci. III 174, 336–359. https://doi.org/10.1016/j.icarus.2004.07.030

Mangold, N., Kite, E.S., Kleinhans, M.G., Newsom, H., Ansan, V., Hauber, E., Kraal, E., Quantin, C., Tanaka, K., 2012. The origin and timing of fluvial activity at Eberswalde crater, Mars. Icarus 220, 530–551. https://doi.org/10.1016/j.icarus.2012.05.026

Marra, W.A., McLelland, S.J., Parsons, D.R., Murphy, B.J., Hauber, E., Kleinhans, M.G., 2015. Groundwater seepage landscapes from distant and local sources in experiments and on Mars. Earth Surf Dynam 3, 389–408. https://doi.org/10.5194/esurf-3-389-2015

Mastrogiuseppe, M., Poggiali, V., Hayes, A.G., Lunine, J.I., Seu, R., Mitri, G., Lorenz, R.D., 2019. Deep and methane-rich lakes on Titan. Nat. Astron. 3, 535–542. https://doi.org/10.1038/s41550-019-0714-2

Masursky, H., 1973. An overview of geological results from Mariner 9. J. Geophys. Res. 78, 4009–4030. https://doi.org/10.1029/JB078i020p04009
McEwen, A.S., 1998. High-Temperature Silicate Volcanism on Jupiter's Moon Io. Science 281, 87–90. https://doi.org/10.1126/science.281.5373.87
McEwen, A.S., 1989. Mobility of large rock avalanches: Evidence from Valles Marineris, Mars. Geology 17, 1111–1114. https://doi.org/10.1130/0091-7613(1989)017<1111:MOLRAE>2.3.CO;2
McEwen, A.S., Ojha, L., Dundas, C.M., Mattson, S.S., Byrne, S., Wray, J.J., Cull, S.C., Murchie, S.L., Thomas, N., Gulick, V.C., 2011. Seasonal Flows on Warm Martian Slopes. Science 333, 740–743. https://doi.org/10.1126/science.1204816
Mellon, M.T., Arvidson, R.E., Sizemore, H.G., Searls, M.L., Blaney, D.L., Cull, S., Hecht, M.H., Heet, T.L., Keller, H.U., Lemmon, M.T., Markiewicz, W.J., Ming, D.W., Morris, R.V., Pike, W.T., Zent, A.P., 2009. Ground ice at the Phoenix Landing Site: Stability state and origin. J. Geophys. Res. Planets 114, E00E07. https://doi.org/10.1029/2009JE003417
Melosh, H.J., 1989. Impact cratering: a geologic process, Oxford monographs on geology and geophysics ; no. 11. Oxford University Press.
Michael, G.G., Neukum, G., 2010. Planetary surface dating from crater size–frequency distribution measurements: Partial resurfacing events and statistical age uncertainty. Earth Planet. Sci. Lett. 294, 223–229. https://doi.org/10.1016/j.epsl.2009.12.041
Miyamoto, H., 2004. Fluid dynamical implications of anastomosing slope streaks on Mars. J. Geophys. Res. 109. https://doi.org/10.1029/2003JE002234
Molaro, J., Byrne, S., 2012. Rates of temperature change of airless landscapes and implications for thermal stress weathering. J Geophys Res 117, E10011. https://doi.org/10.1029/2012JE004138
Moore, J.M., Asphaug, E., Morrison, D., Spencer, J.R., Chapman, C.R., Bierhaus, B., Sullivan, R.J., Chuang, F.C., Klemaszewski, J.E., Greeley, R., Bender, K.C., Geissler, P.E., Helfenstein, P., Pilcher, C.B., 1999. Mass Movement and Landform Degradation on the Icy Galilean Satellites: Results of the Galileo Nominal Mission. Icarus 140, 294–312. https://doi.org/10.1006/icar.1999.6132
Moore, J.M., Howard, A.D., 2010. Are the basins of Titan's Hotei Regio and Tui Regio sites of former low latitude seas?: FORMER LOW LATITUDE SEAS OF TITAN. Geophys. Res. Lett. 37, n/a-n/a. https://doi.org/10.1029/2010GL045234
Moore, J.M., Howard, A.D., Umurhan, O.M., White, O.L., Schenk, P.M., Beyer, R.A., McKinnon, W.B., Spencer, J.R., Singer, K.N., Grundy, W.M., Earle, A.M., Schmitt, B., Protopapa, S., Nimmo, F., Cruikshank, D.P., Hinson, D.P., Young, L.A., Stern, S.A., Weaver, H.A., Olkin, C.B., Ennico, K., Collins, G., Bertrand, T., Forget, F., Scipioni, F., 2018. Bladed Terrain on Pluto: Possible origins and evolution. Icarus 300, 129–144. https://doi.org/10.1016/j.icarus.2017.08.031
Morris, E.C., 1982. Aureole deposits of the Martian volcano Olympus Mons. J. Geophys. Res. 87, 1164–1178.
Mottola, S., Arnold, G., Grothues, H.-G., Jaumann, R., Michaelis, H., Neukum, G., Bibring, J.-P., Schroder, S.E., Hamm, M., Otto, K.A., Pelivan, I., Proffe, G., Scholten, F., Tirsch, D., Kreslavsky, M., Remetean, E., Souvannavong, F., Dolives, B., 2015. The structure of the regolith on 67P/Churyumov-Gerasimenko from ROLIS descent imaging. Science 349, aab0232–aab0232. https://doi.org/10.1126/science.aab0232
Mustard, J.F., Cooper, C.D., Rifkin, M.K., 2001. Evidence for recent climate change on Mars from the identification of youthful near-surface ground ice. Nature 412, 411–414. https://doi.org/10.1038/35086515
Nahm, A.L., Schultz, R.A., 2011. Magnitude of global contraction on Mars from analysis of surface faults: Implications for martian thermal history. Icarus 211, 389–400. https://doi.org/10.1016/j.icarus.2010.11.003
Nathues, A., Schmedemann, N., Thangjam, G., Pasckert, J.H., Mengel, K., Castillo-Rogez, J., Cloutis, E.A., Hiesinger, H., Hoffmann, M., Le Corre, L., Li, J.-Y., Pieters, C., Raymond, C.A., Reddy, V.,

Ruesch, O., Williams, D.A., 2020. Recent cryovolcanic activity at Occator crater on Ceres. Nat. Astron. 4, 794–801. https://doi.org/10.1038/s41550-020-1146-8
Nittler, L.R., Weider, S.Z., 2019. The Surface Composition of Mercury. Elements 15, 33–38. https://doi.org/10.2138/gselements.15.1.33
Obleitner, F., Spötl, C., 2011. The mass and energy balance of ice within the Eisriesenwelt cave, Austria. The Cryosphere 5, 245–257. https://doi.org/10.5194/tc-5-245-2011
Oehler, D.Z., Allen, C.C., 2010. Evidence for pervasive mud volcanism in Acidalia Planitia, Mars. Icarus 208, 636–657. https://doi.org/10.1016/j.icarus.2010.03.031
Ojha, L., McEwen, A., Dundas, C., Byrne, S., Mattson, S., Wray, J., Masse, M., Schaefer, E., 2014. HiRISE observations of Recurring Slope Lineae (RSL) during southern summer on Mars. Icarus 231, 365–376. https://doi.org/10.1016/j.icarus.2013.12.021
Osinski, G.R., Tornabene, L.L., Banerjee, N.R., Cockell, C.S., Flemming, R., Izawa, M.R.M., McCutcheon, J., Parnell, J., Preston, L.J., Pickersgill, A.E., Pontefract, A., Sapers, H.M., Southam, G., 2013. Impact-generated hydrothermal systems on Earth and Mars. Icarus 224, 347–363. https://doi.org/10.1016/j.icarus.2012.08.030
Paillou, P., Seignovert, B., Radebaugh, J., Wall, S., 2016. Radar scattering of linear dunes and mega-yardangs: Application to Titan. Icarus 270, 211–221. https://doi.org/10.1016/j.icarus.2015.07.038
Parker, T.J., Gorsline, D.S., Saunders, R.S., Pieri, D.C., Schneeberger, D.M., 1993. Coastal geomorphology of the Martian northern plains. J. Geophys. Res. 98, 11061. https://doi.org/10.1029/93JE00618
Parsons, R.A., Nimmo, F., Miyamoto, H., 2011. Constraints on martian lobate debris apron evolution and rheology from numerical modeling of ice flow. Icarus 214, 246–257. https://doi.org/10.1016/j.icarus.2011.04.014
Peale, S.J., Schubert, G., Lingenfelter, R.E., 1968. Distribution of Sinuous Rilles and Water on the Moon. Nature 220, 1222–1225. https://doi.org/10.1038/2201222a0
Perron, J.T., Lamb, M.P., Koven, C.D., Fung, I.Y., Yager, E., Ádámkovics, M., 2006. Valley formation and methane precipitation rates on Titan. J. Geophys. Res. 111, E11001. https://doi.org/10.1029/2005JE002602
Petersen, E.I., Holt, J.W., Levy, J.S., 2018. High Ice Purity of Martian Lobate Debris Aprons at the Regional Scale: Evidence From an Orbital Radar Sounding Survey in Deuteronilus and Protonilus Mensae. Geophys. Res. Lett. 45, 11,595-11,604. https://doi.org/10.1029/2018GL079759
Plaut, J.J., Safaeinili, A., Holt, J.W., Phillips, R.J., Head, J.W., Seu, R., Putzig, N.E., Frigeri, A., 2009. Radar evidence for ice in lobate debris aprons in the mid-northern latitudes of Mars. Geophys. Res. Lett. 36, 02203. https://doi.org/10.1029/2008GL036379
Pollack, J.B., Kasting, J.F., Richardson, S.M., Poliakoff, K., 1987. The case for a wet, warm climate on early Mars. Icarus 71, 203–224. https://doi.org/10.1016/0019-1035(87)90147-3
Porco, C.C., Baker, E., Barbara, J., Beurle, K., Brahic, A., Burns, J.A., Charnoz, S., Cooper, N., Dawson, D.D., Del Genio, A.D., Denk, T., Dones, L., Dyudina, U., Evans, M.W., Fussner, S., Giese, B., Grazier, K., Helfenstein, P., Ingersoll, A.P., Jacobson, R.A., Johnson, T.V., McEwen, A., Murray, C.D., Neukum, G., Owen, W.M., Perry, J., Roatsch, T., Spitale, J., Squyres, S., Thomas, P., Tiscareno, M., Turtle, E.P., Vasavada, A.R., Veverka, J., Wagner, R., West, R., 2005. Imaging of Titan from the Cassini spacecraft. Nature 434, 159–168. https://doi.org/10.1038/nature03436
Portyankina, G., Markiewicz, W.J., Thomas, N., Hansen, C.J., Milazzo, M., 2010. HiRISE observations of gas sublimation-driven activity in Mars' southern polar regions: III. Models of processes involving translucent ice. MROHiRISE Stud. Mars 205, 311–320. https://doi.org/10.1016/j.icarus.2009.08.029
Poulos, M.J., Pierce, J.L., Flores, A.N., Benner, S.G., 2012. Hillslope asymmetry maps reveal widespread, multi-scale organization: MAPPING HILLSLOPE ASYMMETRY. Geophys. Res. Lett. 39, n/a-n/a. https://doi.org/10.1029/2012GL051283

Quantin, C., Flahaut, J., Clenet, H., Allemand, P., Thomas, P., 2012. Composition and structures of the subsurface in the vicinity of Valles Marineris as revealed by central uplifts of impact craters. Icarus 221, 436–452. https://doi.org/10.1016/j.icarus.2012.07.031

Reiss, D., Raack, J., Rossi, A.P., Di Achille, G., Hiesinger, H., 2010. First in-situ analysis of dust devil tracks on Earth and their comparison with tracks on Mars: DARK DUST DEVIL TRACKS ON EARTH. Geophys. Res. Lett. 37, n/a-n/a. https://doi.org/10.1029/2010GL044016

Roberts, G.P., Matthews, B., Bristow, C., Guerrieri, L., Vetterlein, J., 2012. Possible evidence of paleomarsquakes from fallen boulder populations, Cerberus Fossae, Mars. J. Geophys. Res. Planets 117, E02009. https://doi.org/10.1029/2011JE003816

Rodriguez, J.A.P., Fairén, A.G., Tanaka, K.L., Zarroca, M., Linares, R., Platz, T., Komatsu, G., Miyamoto, H., Kargel, J.S., Yan, J., Gulick, V., Higuchi, K., Baker, V.R., Glines, N., 2016. Tsunami waves extensively resurfaced the shorelines of an early Martian ocean. Sci. Rep. 6, 25106. https://doi.org/10.1038/srep25106

Rodriguez, J.A.P., Leonard, G.J., Kargel, J.S., Domingue, D., Berman, D.C., Banks, M., Zarroca, M., Linares, R., Marchi, S., Baker, V.R., Webster, K.D., Sykes, M., 2020. The Chaotic Terrains of Mercury Reveal a History of Planetary Volatile Retention and Loss in the Innermost Solar System. Sci. Rep. 10, 4737. https://doi.org/10.1038/s41598-020-59885-5

Ruesch, O., Sefton-Nash, E., Vago, J.L., Küppers, M., Pasckert, J.H., Krohn, K., Otto, K., 2020. In situ fragmentation of lunar blocks and implications for impacts and solar-induced thermal stresses. Icarus 336, 113431. https://doi.org/10.1016/j.icarus.2019.113431

Ryan, J.A., Lucich, R.D., 1983. Possible dust devils, vortices on Mars. J. Geophys. Res. 88, 11005. https://doi.org/10.1029/JC088iC15p11005

Sasaki, S., Honda, C., Sugita, S., Miyammoto, H., Michikami, T., Morota, T., Kanda, S., Kikuchi, H., 2021. Crack orientations of boulders and thermal fatigue on (162173) Ryugu. 43rd COSPAR Sci. Assem. Held 28 January-4 Febr. 43, 270.

Sauro, F., Pozzobon, R., Massironi, M., De Berardinis, P., Santagata, T., De Waele, J., 2020. Lava tubes on Earth, Moon and Mars: A review on their size and morphology revealed by comparative planetology. Earth-Sci. Rev. 209, 103288. https://doi.org/10.1016/j.earscirev.2020.103288

Schenk, P., Jackson, M.P.A., 1993. Diapirism on Triton: A record of crustal layering and instability. Geology 21, 299–302.

Schleicher, L.S., Watters, T.R., Martin, A.J., Banks, M.E., 2019. Wrinkle ridges on Mercury and the Moon within and outside of mascons. Icarus 331, 226–237. https://doi.org/10.1016/j.icarus.2019.04.013

Schmidt, B.E., Hughson, K.H.G., Chilton, H.T., Scully, J.E.C., Platz, T., Nathues, A., Sizemore, H., Bland, M.T., Byrne, S., Marchi, S., O'Brien, D.P., Schorghofer, N., Hiesinger, H., Jaumann, R., Pasckert, J.H., Lawrence, J.D., Buzckowski, D., Castillo-Rogez, J.C., Sykes, M.V., Schenk, P.M., DeSanctis, M.-C., Mitri, G., Formisano, M., Li, J.-Y., Reddy, V., LeCorre, L., Russell, C.T., Raymond, C.A., 2017. Geomorphological evidence for ground ice on dwarf planet Ceres. Nat. Geosci. 10, 338–343. https://doi.org/10.1038/ngeo2936

Schmidt, F., Andrieu, F., Costard, F., Kocifaj, M., Meresescu, A.G., 2017. Formation of recurring slope lineae on Mars by rarefied gas-triggered granular flows. Nat. Geosci 10, 270–273.

Schorghofer, N., Aharonson, O., Gerstell, M.F., Tatsumi, L., 2007. Three decades of slope streak activity on Mars. Icarus 191, 132–140. https://doi.org/10.1016/j.icarus.2007.04.026

Schultz, P.H., Gault, D.E., 1975. Seismic effects from major basin formations on the moon and mercury. The Moon 12, 159–177. https://doi.org/10.1007/BF00577875

Scully, J.E.C., Russell, C.T., Yin, A., Jaumann, R., Carey, E., Castillo-Rogez, J., McSween, H.Y., Raymond, C.A., Reddy, V., Le Corre, L., 2015. Geomorphological evidence for transient water flow on Vesta. Earth Planet. Sci. Lett. 411, 151–163. https://doi.org/10.1016/j.epsl.2014.12.004

Sefton-Nash, E., Catling, D.C., Wood, S.E., Grindrod, P.M., Teanby, N.A., 2012. Topographic, spectral and thermal inertia analysis of interior layered deposits in Iani Chaos, Mars. Icarus 221, 20–42. https://doi.org/10.1016/j.icarus.2012.06.036

1087 Séjourné, A., Costard, F., Gargani, J., Soare, R.J., Fedorov, A., Marmo, C., 2011. Scalloped depressions
1088 and small-sized polygons in western Utopia Planitia, Mars: A new formation hypothesis.
1089 Planet. Space Sci. 59, 412–422. https://doi.org/10.1016/j.pss.2011.01.007
1090 Senthil Kumar, P., Keerthi, V., Senthil Kumar, A., Mustard, J., Gopala Krishna, B., Amitabh, Ostrach,
1091 L.R., Kring, David.A., Kiran Kumar, A.S., Goswami, J.N., 2013. Gullies and landslides on the
1092 Moon: Evidence for dry-granular flows. J. Geophys. Res. Planets 118, 206–223.
1093 https://doi.org/10.1002/jgre.20043
1094 Senthil Kumar, P., Sruthi, U., Krishna, N., Lakshmi, K.J.P., Menon, R., Amitabh, Gopala Krishna, B.,
1095 Kring, D.A., Head, J.W., Goswami, J.N., Kiran Kumar, A.S., 2016. Recent shallow moonquake
1096 and impact-triggered boulder falls on the Moon: New insights from the Schrödinger basin:
1097 Recent Seismotectonics of the Moon. J. Geophys. Res. Planets.
1098 https://doi.org/10.1002/2015JE004850
1099 Sharp, R.P., 1980. Geomorphological Processes on Terrestrial Planetary Surfaces. Annu. Rev. Earth
1100 Planet. Sci. 8, 231–261. https://doi.org/10.1146/annurev.ea.08.050180.001311
1101 Sholes, S.F., Dickeson, Z.I., Montgomery, D.R., Catling, D.C., 2021. Where are Mars' Hypothesized
1102 Ocean Shorelines? Large Lateral and Topographic Offsets Between Different Versions of
1103 Paleoshoreline Maps. J. Geophys. Res. Planets 126. https://doi.org/10.1029/2020JE006486
1104 Singer, K.N., McKinnon, W.B., Schenk, P.M., Moore, J.M., 2012. Massive ice avalanches on Iapetus
1105 mobilized by friction reduction during flash heating. Nat. Geosci. 5, 574–578.
1106 https://doi.org/10.1038/ngeo1526
1107 Skjetne, H.L., Singer, K.N., Hynek, B.M., Knight, K.I., Schenk, P.M., Olkin, C.B., White, O.L., Bertrand,
1108 T., Runyon, K.D., McKinnon, W.B., Moore, J.M., Stern, S.A., Weaver, H.A., Young, L.A., Ennico,
1109 K., 2021. Morphological comparison of blocks in chaos terrains on Pluto, Europa, and Mars.
1110 Icarus 356, 113866. https://doi.org/10.1016/j.icarus.2020.113866
1111 Soare, R.J., Burr, D.M., Wan Bun Tseung, J.M., 2005. Possible pingos and a periglacial landscape in
1112 northwest Utopia Planitia. Icarus 174, 373–382. https://doi.org/10.1016/j.icarus.2004.11.013
1113 Soare, R.J., Conway, S.J., Dohm, J.M., 2014. Possible ice-wedge polygons and recent landscape
1114 modification by "wet" periglacial processes in and around the Argyre impact basin, Mars.
1115 Icarus 233, 214–228. https://doi.org/10.1016/j.icarus.2014.01.034
1116 Soare, R.J., Conway, S.J., Gallagher, C., Dohm, J.M., 2016. Sorted (clastic) polygons in the Argyre
1117 region, Mars, and possible evidence of pre- and post-glacial periglaciation in the Late
1118 Amazonian Epoch. Icarus 264, 184–197. https://doi.org/10.1016/j.icarus.2015.09.019
1119 Soare, R.J., Conway, S.J., Williams, J.-P., Philippe, M., Mc Keown, L.E., Godin, E., Hawkswell, J., 2021.
1120 Possible ice-wedge polygonisation in Utopia Planitia, Mars and its latitudinal gradient of
1121 distribution. Icarus 358, 114208. https://doi.org/10.1016/j.icarus.2020.114208
1122 Soare, R.J., Kargel, J.S., Osinski, G.R., Costard, F., 2007. Thermokarst processes and the origin of
1123 crater-rim gullies in Utopia and western Elysium Planitia. Icarus 191, 95–112.
1124 Soare, R.J., Osinski, G.R., Roehm, C.L., 2008. Thermokarst lakes and ponds on Mars in the very recent
1125 (late Amazonian) past. Earth Planet. Sci. Lett. 272, 382–393.
1126 https://doi.org/10.1016/j.epsl.2008.05.010
1127 Soderblom, L.A., 1970. A model for small-impact erosion applied to the lunar surface. J. Geophys.
1128 Res. 75, 2655–2661. https://doi.org/10.1029/JB075i014p02655
1129 Stein, N., Grotzinger, J.P., Schieber, J., Mangold, N., Hallet, B., Newsom, H., Stack, K.M., Berger, J.A.,
1130 Thompson, L., Siebach, K.L., Cousin, A., Le Mouélic, S., Minitti, M., Sumner, D.Y., Fedo, C.,
1131 House, C.H., Gupta, S., Vasavada, A.R., Gellert, R., Wiens, R.C., Frydenvang, J., Forni, O.,
1132 Meslin, P.Y., Payré, V., Dehouck, E., 2018. Desiccation cracks provide evidence of lake drying
1133 on Mars, Sutton Island member, Murray formation, Gale Crater. Geology 46, 515–518.
1134 https://doi.org/10.1130/G40005.1
1135 Stern, S.A., Binzel, R.P., Earle, A.M., Singer, K.N., Young, L.A., Weaver, H.A., Olkin, C.B., Ennico, K.,
1136 Moore, J.M., McKinnon, W.B., Spencer, J.R., 2017. Past epochs of significantly higher
1137 pressure atmospheres on Pluto. Icarus 287, 47–53.
1138 https://doi.org/10.1016/j.icarus.2016.11.022

Stillman, D.E., Bue, B.D., Wagstaff, K.L., Primm, K.M., Michaels, T.I., Grimm, R.E., 2020. Evaluation of wet and dry recurring slope lineae (RSL) formation mechanisms based on quantitative mapping of RSL in Garni Crater, Valles Marineris, Mars. Icarus 335, 113420. https://doi.org/10.1016/j.icarus.2019.113420

Stuart-Alexander, D.E., Howard, K.A., 1970. Lunar Maria and circular basins—a review. Icarus 12, 440–456. https://doi.org/10.1016/0019-1035(70)90013-8

Sullivan, R., Kok, J.F., Katra, I., Yizhaq, H., 2020. A Broad Continuum of Aeolian Impact Ripple Morphologies on Mars is Enabled by Low Wind Dynamic Pressures. J. Geophys. Res. Planets 125. https://doi.org/10.1029/2020JE006485

Sullivan, R., Thomas, P., Veverka, J., Malin, M., Edgett, K.S., 2001. Mass movement slope streaks imaged by the Mars Orbiter Camera. J Geophys Res-Planets 106, 23607–23633.

Telfer, M.W., Parteli, E.J.R., Radebaugh, J., Beyer, R.A., Bertrand, T., Forget, F., Nimmo, F., Grundy, W.M., Moore, J.M., Stern, S.A., Spencer, J., Lauer, T.R., Earle, A.M., Binzel, R.P., Weaver, H.A., Olkin, C.B., Young, L.A., Ennico, K., Runyon, K., The New Horizons Geology, Geophysics and Imaging Science Theme Team, Buie, M., Buratti, B., Cheng, A., Kavelaars, J.J., Linscott, I., McKinnon, W.B., Reitsema, H., Reuter, D., Schenk, P., Showalter, M., Tyler, L., 2018. Dunes on Pluto. Science 360, 992–997. https://doi.org/10.1126/science.aao2975

Tesson, P.-A., Conway, S.J., Mangold, N., Ciazela, J., Lewis, S.R., Mège, D., 2020. Evidence for thermal-stress-induced rockfalls on Mars impact crater slopes. Icarus 342, 113503. https://doi.org/10.1016/j.icarus.2019.113503

Thomas, N., Davidsson, B., El-Maarry, M.R., Fornasier, S., Giacomini, L., Gracia-Berná, A.G., Hviid, S.F., Ip, W.-H., Jorda, L., Keller, H.U., Knollenberg, J., Kührt, E., La Forgia, F., Lai, I.L., Liao, Y., Marschall, R., Massironi, M., Mottola, S., Pajola, M., Poch, O., Pommerol, A., Preusker, F., Scholten, F., Su, C.C., Wu, J.S., Vincent, J.-B., Sierks, H., Barbieri, C., Lamy, P.L., Rodrigo, R., Koschny, D., Rickman, H., A'Hearn, M.F., Barucci, M.A., Bertaux, J.-L., Bertini, I., Cremonese, G., Da Deppo, V., Debei, S., de Cecco, M., Fulle, M., Groussin, O., Gutierrez, P.J., Kramm, J.-R., Küppers, M., Lara, L.M., Lazzarin, M., Lopez Moreno, J.J., Marzari, F., Michalik, H., Naletto, G., Agarwal, J., Güttler, C., Oklay, N., Tubiana, C., 2015. Redistribution of particles across the nucleus of comet 67P/Churyumov-Gerasimenko. Astron. Astrophys. 583, A17. https://doi.org/10.1051/0004-6361/201526049

Thomas, N., Portyankina, G., Hansen, C.J., Pommerol, A., 2011. HiRISE observations of gas sublimation-driven activity in Mars' southern polar regions: IV. Fluid dynamics models of CO2 jets. Icarus 212, 66–85. https://doi.org/10.1016/j.icarus.2010.12.016

Thomas, P., Gierasch, P.J., 1985. Dust Devils on Mars. Science 230, 175–177. https://doi.org/10.1126/science.230.4722.175

Thomas, R.J., Rothery, D.A., Conway, S.J., Anand, M., 2014. Long-lived explosive volcanism on Mercury. Geophys. Res. Lett. 41, 6084–6092. https://doi.org/10.1002/2014GL061224

Thomson, B.J., Bridges, N.T., Greeley, R., 2008. Rock abrasion features in the Columbia Hills, Mars. J. Geophys. Res. 113, E08010. https://doi.org/10.1029/2007JE003018

Tomasko, M.G., Archinal, B., Becker, T., Bézard, B., Bushroe, M., Combes, M., Cook, D., Coustenis, A., de Bergh, C., Dafoe, L.E., Doose, L., Douté, S., Eibl, A., Engel, S., Gliem, F., Grieger, B., Holso, K., Howington-Kraus, E., Karkoschka, E., Keller, H.U., Kirk, R., Kramm, R., Küppers, M., Lanagan, P., Lellouch, E., Lemmon, M., Lunine, J., McFarlane, E., Moores, J., Prout, G.M., Rizk, B., Rosiek, M., Rueffer, P., Schröder, S.E., Schmitt, B., See, C., Smith, P., Soderblom, L., Thomas, N., West, R., 2005. Rain, winds and haze during the Huygens probe's descent to Titan's surface. Nature 438, 765–778. https://doi.org/10.1038/nature04126

van den Broeke, M.R., Bintanja, R., 1995. Summertime atmospheric circulation in the vicinity of a blue ice area in Queen Maud Land, Antarctica. Bound.-Layer Meteorol. 72, 411–438. https://doi.org/10.1007/BF00709002

Veeder, G.J., Davies, A.G., Matson, D.L., Johnson, T.V., 2009. Io: Heat flow from dark volcanic fields. Icarus 204, 239–253. https://doi.org/10.1016/j.icarus.2009.06.027

Vijayan, S., Harish, Kimi, K., Tuhi, S., Vigneshwaran, K., Sinha, R., Conway, S.J., Sivaraman, B., Bhardwaj, A., 2021. Boulder Fall Ejecta: Present day activity on Mars. Geophys. Res. Lett. Accepted.

Vincent, J.-B., Bodewits, D., Besse, S., Sierks, H., Barbieri, C., Lamy, P., Rodrigo, R., Koschny, D., Rickman, H., Keller, H.U., Agarwal, J., A'Hearn, M.F., Auger, A.-T., Barucci, M.A., Bertaux, J.-L., Bertini, I., Capanna, C., Cremonese, G., Da Deppo, V., Davidsson, B., Debei, S., De Cecco, M., El-Maarry, M.R., Ferri, F., Fornasier, S., Fulle, M., Gaskell, R., Giacomini, L., Groussin, O., Guilbert-Lepoutre, A., Gutierrez-Marques, P., Gutierrez, P.J., Guttler, C., Hoekzema, N., Hofner, S., Hviid, S.F., Ip, W.-H., Jorda, L., Knollenberg, J., Kovacs, G., Kramm, R., Kuhrt, E., Kuppers, M., La Forgia, F., Lara, L.M., Lazzarin, M., Lee, V., Leyrat, C., Lin, Z.-Y., Lopez Moreno, J.J., Lowry, S., Magrin, S., Maquet, L., Marchi, S., Marzari, F., Massironi, M., Michalik, H., Moissl, R., Mottola, S., Naletto, G., Oklay, N., Pajola, M., Preusker, F., Scholten, F., Thomas, N., Toth, I., Tubiana, C., 2015. Large heterogeneities in comet 67P as revealed by active pits from sinkhole collapse. Nature 523, 63–66. https://doi.org/10.1038/nature14564

Vincent, J.-B., Oklay, N., Pajola, M., Höfner, S., Sierks, H., Hu, X., Barbieri, C., Lamy, P.L., Rodrigo, R., Koschny, D., Rickman, H., Keller, H.U., A'Hearn, M.F., Barucci, M.A., Bertaux, J.-L., Bertini, I., Besse, S., Bodewits, D., Cremonese, G., Da Deppo, V., Davidsson, B., Debei, S., De Cecco, M., El-Maarry, M.R., Fornasier, S., Fulle, M., Groussin, O., Gutiérrez, P.J., Gutiérrez-Marquez, P., Güttler, C., Hofmann, M., Hviid, S.F., Ip, W.-H., Jorda, L., Knollenberg, J., Kovacs, G., Kramm, J.-R., Kührt, E., Küppers, M., Lara, L.M., Lazzarin, M., Lin, Z.-Y., Lopez Moreno, J.J., Lowry, S., Marzari, F., Massironi, M., Moreno, F., Mottola, S., Naletto, G., Preusker, F., Scholten, F., Shi, X., Thomas, N., Toth, I., Tubiana, C., 2016. Are fractured cliffs the source of cometary dust jets? Insights from OSIRIS/Rosetta at 67P/Churyumov-Gerasimenko. Astron. Astrophys. 587, A14. https://doi.org/10.1051/0004-6361/201527159

Viola, D., McEwen, A.S., Dundas, C.M., Byrne, S., 2015. Expanded secondary craters in the Arcadia Planitia region, Mars: Evidence for tens of Myr-old shallow subsurface ice. Icarus 248, 190–204. https://doi.org/10.1016/j.icarus.2014.10.032

Walsh, K.J., Jawin, E.R., Ballouz, R.-L., Barnouin, O.S., Bierhaus, E.B., Connolly, H.C., Molaro, J.L., McCoy, T.J., Delbo', M., Hartzell, C.M., Pajola, M., Schwartz, S.R., Trang, D., Asphaug, E., Becker, K.J., Beddingfield, C.B., Bennett, C.A., Bottke, W.F., Burke, K.N., Clark, B.C., Daly, M.G., DellaGiustina, D.N., Dworkin, J.P., Elder, C.M., Golish, D.R., Hildebrand, A.R., Malhotra, R., Marshall, J., Michel, P., Nolan, M.C., Perry, M.E., Rizk, B., Ryan, A., Sandford, S.A., Scheeres, D.J., Susorney, H.C.M., Thuillet, F., Lauretta, D.S., The OSIRIS-REx Team, 2019. Craters, boulders and regolith of (101955) Bennu indicative of an old and dynamic surface. Nat. Geosci. 12, 242–246. https://doi.org/10.1038/s41561-019-0326-6

Warner, N., Gupta, S., Muller, J.-P., Kim, J.-R., Lin, S.-Y., 2009. A refined chronology of catastrophic outflow events in Ares Vallis, Mars. Earth Planet. Sci. Lett. 288, 58–69.

Watters, T.R., Robinson, M.S., Beyer, R.A., Banks, M.E., Bell, J.F., Pritchard, M.E., Hiesinger, H., van der Bogert, C.H., Thomas, P.C., Turtle, E.P., Williams, N.R., 2010. Evidence of Recent Thrust Faulting on the Moon Revealed by the Lunar Reconnaissance Orbiter Camera. Science 329, 936–940. https://doi.org/10.1126/science.1189590

Wells, G.L., Zimbelman, J.R., 1997. Extraterrestrial arid surface processes. Arid Zone Geomorphol. Process Form Change Drylands.

White, O.L., Umurhan, O.M., Moore, J.M., Howard, A.D., 2016. Modeling of ice pinnacle formation on Callisto: Modeling of Callisto's Pinnacle Terrain. J. Geophys. Res. Planets 121, 21–45. https://doi.org/10.1002/2015JE004846

Williams, R.M.E., Grotzinger, J.P., Dietrich, W.E., Gupta, S., Sumner, D.Y., Wiens, R.C., Mangold, N., Malin, M.C., Edgett, K.S., Maurice, S., Forni, O., Gasnault, O., Ollila, A., Newsom, H.E., Dromart, G., Palucis, M.C., Yingst, R.A., Anderson, R.B., Herkenhoff, K.E., Le Mouelic, S., Goetz, W., Madsen, M.B., Koefoed, A., Jensen, J.K., Bridges, J.C., Schwenzer, S.P., Lewis, K.W., Stack, K.M., Rubin, D., Kah, L.C., Bell, J.F., Farmer, J.D., Sullivan, R., Van Beek, T., Blaney, D.L., Pariser, O., Deen, R.G., MSL Science Team, Kemppinen, O., Bridges, N., Johnson, J.R., Minitti,

M., Cremers, D., Edgar, L., Godber, A., Wadhwa, M., Wellington, D., McEwan, I., Newman, C., Richardson, M., Charpentier, A., Peret, L., King, P., Blank, J., Weigle, G., Schmidt, M., Li, S., Milliken, R., Robertson, K., Sun, V., Baker, M., Edwards, C., Ehlmann, B., Farley, K., Griffes, J., Miller, H., Newcombe, M., Pilorget, C., Rice, M., Siebach, K., Stolper, E., Brunet, C., Hipkin, V., Leveille, R., Marchand, G., Sobron Sanchez, P., Favot, L., Cody, G., Steele, A., Fluckiger, L., Lees, D., Nefian, A., Martin, M., Gailhanou, M., Westall, F., Israel, G., Agard, C., Baroukh, J., Donny, C., Gaboriaud, A., Guillemot, P., Lafaille, V., Lorigny, E., Paillet, A., Perez, R., Saccoccio, M., Yana, C., Aparicio, C.A., Caride Rodriguez, J., Carrasco Blazquez, I., Gomez Gomez, F., Elvira, J.G., Hettrich, S., Lepinette Malvitte, A., Marin Jimenez, M., Frias, J.M., Soler, J.M., Torres, F.J.M., Molina Jurado, A., Sotomayor, L.M., Munoz Caro, G., Navarro Lopez, S., Gonzalez, V.P., Garcia, J.P., Rodriguez Manfredi, J.A., Planello, J.J.R., Alejandra Sans Fuentes, S., Sebastian Martinez, E., Torres Redondo, J., O'Callaghan, R.U., Zorzano Mier, M.-P., Chipera, S., Lacour, J.-L., Mauchien, P., Sirven, J.-B., Manning, H., Fairen, A., Hayes, A., Joseph, J., Squyres, S., Thomas, P., Dupont, A., Lundberg, A., Melikechi, N., Mezzacappa, A., DeMarines, J., Grinspoon, D., Reitz, G., Prats, B., Atlaskin, E., Genzer, M., Harri, A.-M., Haukka, H., Kahanpaa, H., Kauhanen, J., Paton, M., Polkko, J., Schmidt, W., Siili, T., Fabre, C., Wray, J., Wilhelm, M.B., Poitrasson, F., Patel, K., Gorevan, S., Indyk, S., Paulsen, G., Bish, D., Schieber, J., Gondet, B., Langevin, Y., Geffroy, C., Baratoux, D., Berger, G., Cros, A., Uston, C. d., Lasue, J., Lee, Q.-M., Meslin, P.-Y., Pallier, E., Parot, Y., Pinet, P., Schroder, S., Toplis, M., Lewin, E., Brunner, W., Heydari, E., Achilles, C., Oehler, D., Sutter, B., Cabane, M., Coscia, D., Szopa, C., Robert, F., Sautter, V., Nachon, M., Buch, A., Stalport, F., Coll, P., Francois, P., Raulin, F., Teinturier, S., Cameron, J., Clegg, S., Cousin, A., DeLapp, D., Dingler, R., Jackson, R.S., Johnstone, S., Lanza, N., Little, C., Nelson, T., Williams, R.B., Jones, A., Kirkland, L., Treiman, A., Baker, B., Cantor, B., Caplinger, M., Davis, S., Duston, B., Fay, D., Hardgrove, C., Harker, D., Herrera, P., Jensen, E., Kennedy, M.R., Krezoski, G., Krysak, D., Lipkaman, L., McCartney, E., McNair, S., Nixon, B., Posiolova, L., Ravine, M., Salamon, A., Saper, L., Stoiber, K., Supulver, K., Van Beek, J., Zimdar, R., French, K.L., Iagnemma, K., Miller, K., Summons, R., Goesmann, F., Hviid, S., Johnson, M., Lefavor, M., Lyness, E., Breves, E., Dyar, M.D., Fassett, C., Blake, D.F., Bristow, T., DesMarais, D., Edwards, L., Haberle, R., Hoehler, T., Hollingsworth, J., Kahre, M., Keely, L., McKay, C., Bleacher, L., Brinckerhoff, W., Choi, D., Conrad, P., Dworkin, J.P., Eigenbrode, J., Floyd, M., Freissinet, C., Garvin, J., Glavin, D., Harpold, D., Mahaffy, P., Martin, D.K., McAdam, A., Pavlov, A., Raaen, E., Smith, M.D., Stern, J., Tan, F., Trainer, M., Meyer, M., Posner, A., Voytek, M., Anderson, R.C., Aubrey, A., Beegle, L.W., Behar, A., Brinza, D., Calef, F., Christensen, L., Crisp, J.A., DeFlores, L., Feldman, J., Feldman, S., Flesch, G., Hurowitz, J., Jun, I., Keymeulen, D., Maki, J., Mischna, M., Morookian, J.M., Parker, T., Pavri, B., Schoppers, M., Sengstacken, A., Simmonds, J.J., Spanovich, N., de la Torre Juarez, M., Vasavada, A.R., Webster, C.R., Yen, A., Archer, P.D., Cucinotta, F., Jones, J.H., Ming, D., Morris, R.V., Niles, P., Rampe, E., Nolan, T., Fisk, M., Radziemski, L., Barraclough, B., Bender, S., Berman, D., Dobrea, E.N., Tokar, R., Vaniman, D., Leshin, L., Cleghorn, T., Huntress, W., Manhes, G., Hudgins, J., Olson, T., Stewart, N., Sarrazin, P., Grant, J., Vicenzi, E., Wilson, S.A., Bullock, M., Ehresmann, B., Hamilton, V., Hassler, D., Peterson, J., Rafkin, S., Zeitlin, C., Fedosov, F., Golovin, D., Karpushkina, N., Kozyrev, A., Litvak, M., Malakhov, A., Mitrofanov, I., Mokrousov, M., Nikiforov, S., Prokhorov, V., Sanin, A., Tretyakov, V., Varenikov, A., Vostrukhin, A., Kuzmin, R., Clark, B., Wolff, M., McLennan, S., Botta, O., Drake, D., Bean, K., Lemmon, M., Lee, E.M., Sucharski, R., Hernandez, M.A. d. P., Blanco Avalos, J.J., Ramos, M., Kim, M.-H., Malespin, C., Plante, I., Muller, J.-P., Gonzalez, R.N., Ewing, R., Boynton, W., Downs, R., Fitzgibbon, M., Harshman, K., Morrison, S., Kortmann, O., Williams, A., Lugmair, G., Wilson, M.A., Jakosky, B., Zunic, T.B., Frydenvang, J., Kinch, K., Stipp, S.L.S., Boyd, N., Campbell, J.L., Gellert, R., Perrett, G., Pradler, I., VanBommel, S., Jacob, S., Owen, T., Rowland, S., Savijarvi, H., Boehm, E., Bottcher, S., Burmeister, S., Guo, J., Kohler, J., Garcia, C.M., Mellin, R.M., Schweingruber, R.W., McConnochie, T., Benna, M., Franz, H., Bower, H., Brunner, A., Blau, H., Boucher, T., Carmosino, M., Atreya, S., Elliott, H.,

Halleaux, D., Renno, N., Wong, M., Pepin, R., Elliott, B., Spray, J., Thompson, L., Gordon, S., Williams, J., Vasconcelos, P., Bentz, J., Nealson, K., Popa, R., Moersch, J., Tate, C., Day, M., Kocurek, G., Hallet, B., Sletten, R., Francis, R., McCullough, E., Cloutis, E., ten Kate, I.L., Arvidson, R., Fraeman, A., Scholes, D., Slavney, S., Stein, T., Ward, J., Berger, J., Moores, J.E., 2013. Martian Fluvial Conglomerates at Gale Crater. Science 340, 1068–1072. https://doi.org/10.1126/science.1237317

Williams, R.M.E., Irwin, R.P., Zimbelman, J.R., 2009. Evaluation of paleohydrologic models for terrestrial inverted channels: Implications for application to martian sinuous ridges. Geomorphology 107, 300–315. https://doi.org/10.1016/j.geomorph.2008.12.015

Wyrick, D., 2004. Distribution, morphology, and origins of Martian pit crater chains. J. Geophys. Res. 109. https://doi.org/10.1029/2004JE002240

Xiao, Z., Zeng, Z., Ding, N., Molaro, J., 2013. Mass wasting features on the Moon – how active is the lunar surface? Earth Planet. Sci. Lett. 376, 1–11. https://doi.org/10.1016/j.epsl.2013.06.015

Zharkova, A.Yu., Kreslavsky, M.A., Head, J.W., Kokhanov, A.A., 2020. Regolith textures on Mercury: Comparison with the Moon. Icarus 351, 113945. https://doi.org/10.1016/j.icarus.2020.113945

Zimbelman, J.R., Foroutan, M., 2020. Dingo Gap: Curiosity Went Up a Small Transverse Aeolian Ridge and Came Down a Megaripple. J. Geophys. Res. Planets 125. https://doi.org/10.1029/2020JE006489

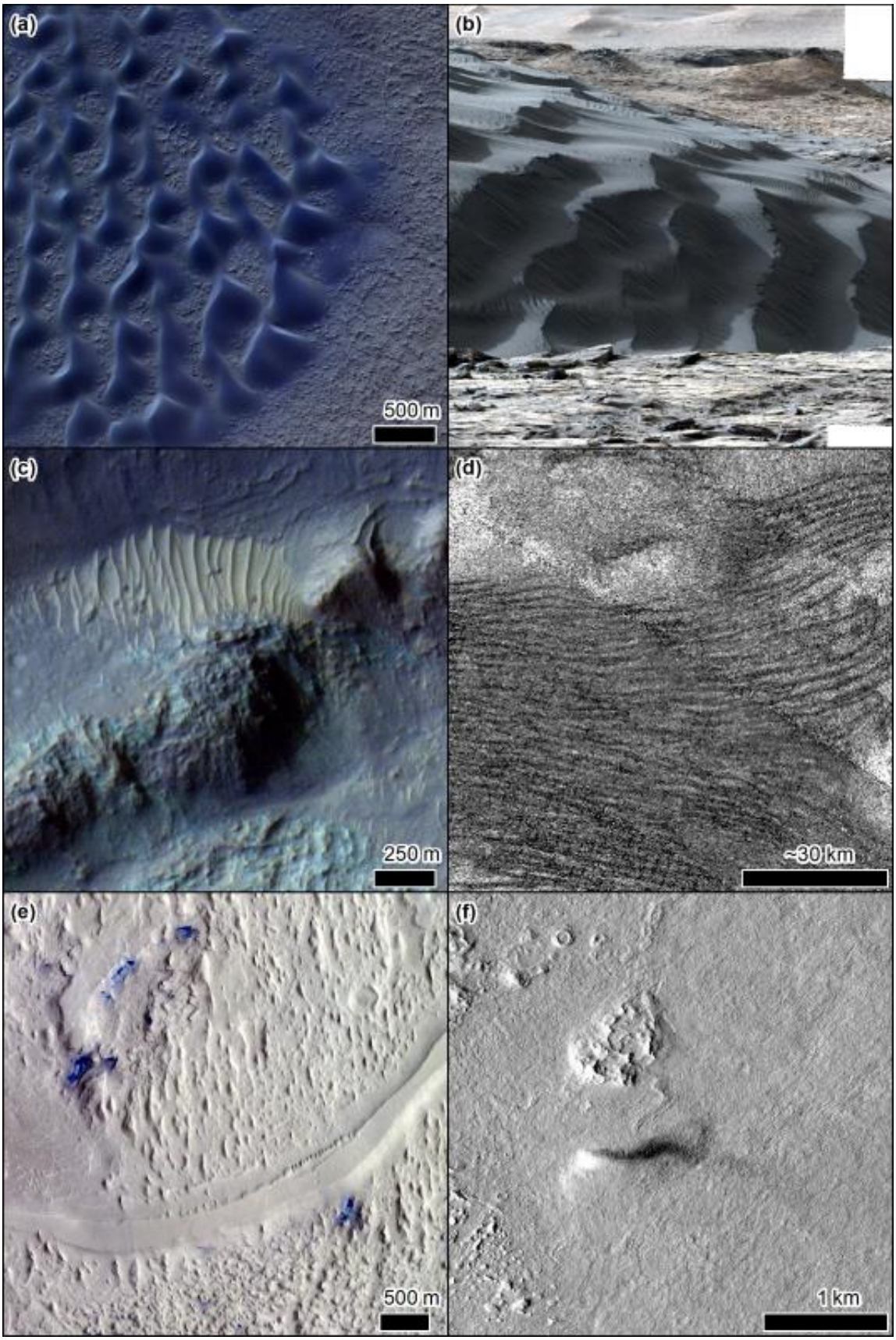

Figure 1: Aeolian planetary landforms. a) Dark Dunefield on the floor of a 35-km-diameter crater in Aonia Terra on Mars (sunlight from the left), CaSSIS image MY36_015406_006_0, credit ESA/Roscosmos/Unibe. b) Large ripples (spacing 2-2.5 m) superposed by smaller impact ripples on

the secondary lee slope of Namib Dune in Gale Crater on Mars (sunlight from the left). Mosaic of MSL Mastcam images from sol 1192 (Ewing et al., 2017), credit NASA/JPL-Caltech/Malin Space Science Systems. c) Transverse aeolian ridges (TARs) on the floor of a 17-km-diameter crater in Margaritifer Terra on Mars (sunlight from the left), CaSSIS image MY36_015406_006_0, credit ESA/Roscosmos/Unibe. (d) Cassini Synthetic Aperture radar image of the Shangri-La Sand Sea on Titan (PIA20710). Image credit NASA/JPL-Caltech/ASI. (e) Yardangs and an inverted channel in Aeolis Mensae region of Mars (sunlight from the right), CaSSIS image MY34_005683_188_2, credit ESA/Roscosmos/Unibe. (f) Dust Devil in Amazonis Planitia on Mars (sunlight from the left), CTX image D02_028082_2155. Credit NASA/JPL/MSSS. North is up in all images apart from (b).

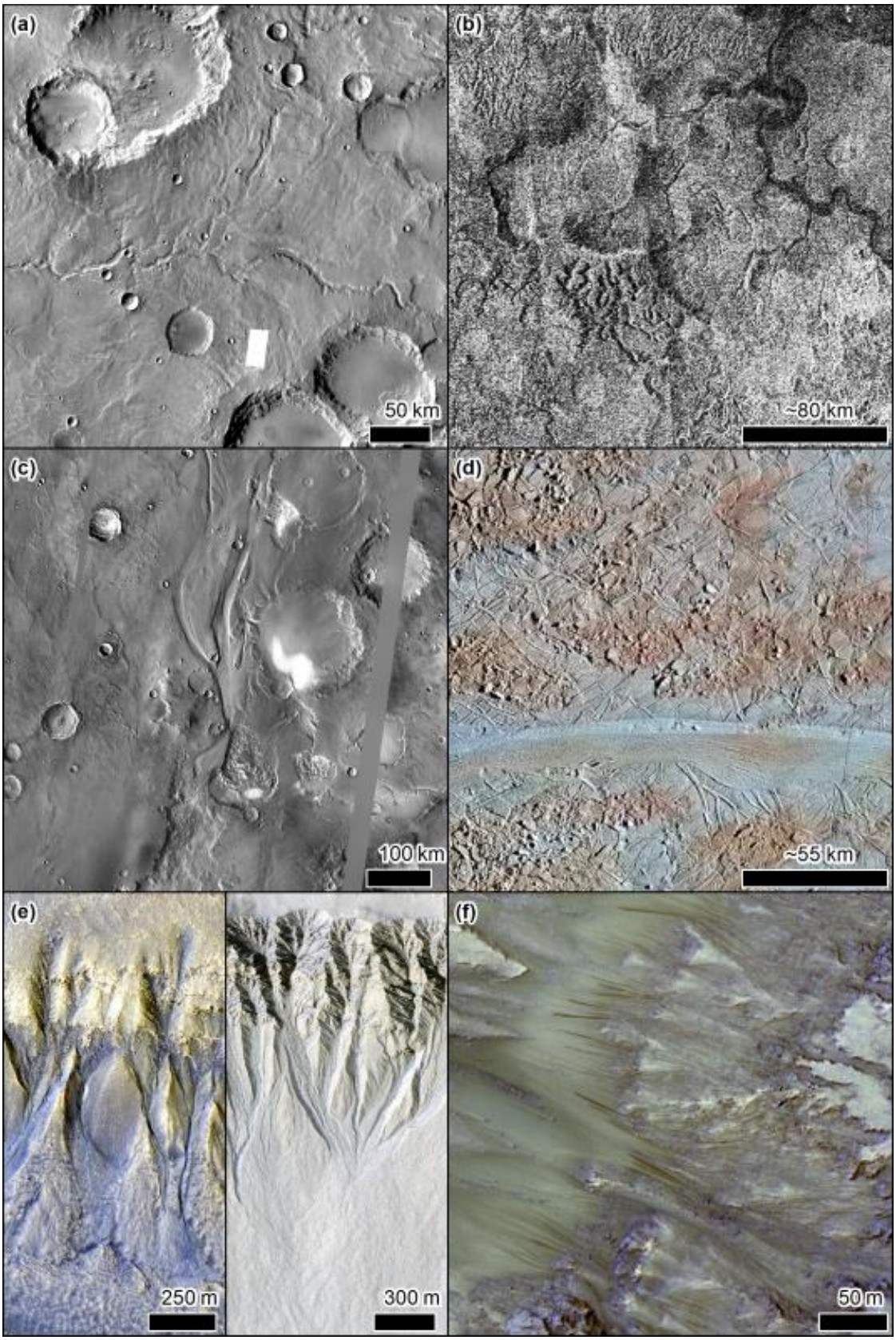

Figure 2: Fluvial planetary landforms. a) Evros Vallis, a valley network in Sinus Sabaeus region of Mars (sunlight from the left). The image is the Day IR THEMIS controlled mosaic available from the USGS. b) A synthetic aperture radar image of valleys near Titan's south pole taken by the Cassini spacecraft image reference PIA10219, credit NASA/JPL-Caltech/ASI. c) Baetis Chaos leading north into Maja

Valles outflow channel on Mars (sunlight from the left). The image is the Day IR THEMIS controlled mosaic available from the USGS. d) Chaos terrain on Europa near Agenor Linea (sunlight from the right) taken by Galileo, image reference PIA23873, credit NASA/JPL-Caltech/SETI Institute. e) Two false-colour images of gullies on Mars (sunlight from the left in both): left Crater in Terra Cimmeria HiRISE image PSP_004019_1420 and right Gasa Crater, HiRISE image PSP_003939_1420, credit NASA/JPL/UofA. f) Recurring Slope Lineae in Palikir Crater (sunlight from the left), HiRISE image ESP_031102_1380, credit NASA/JPL/UofA. North is up in all images.

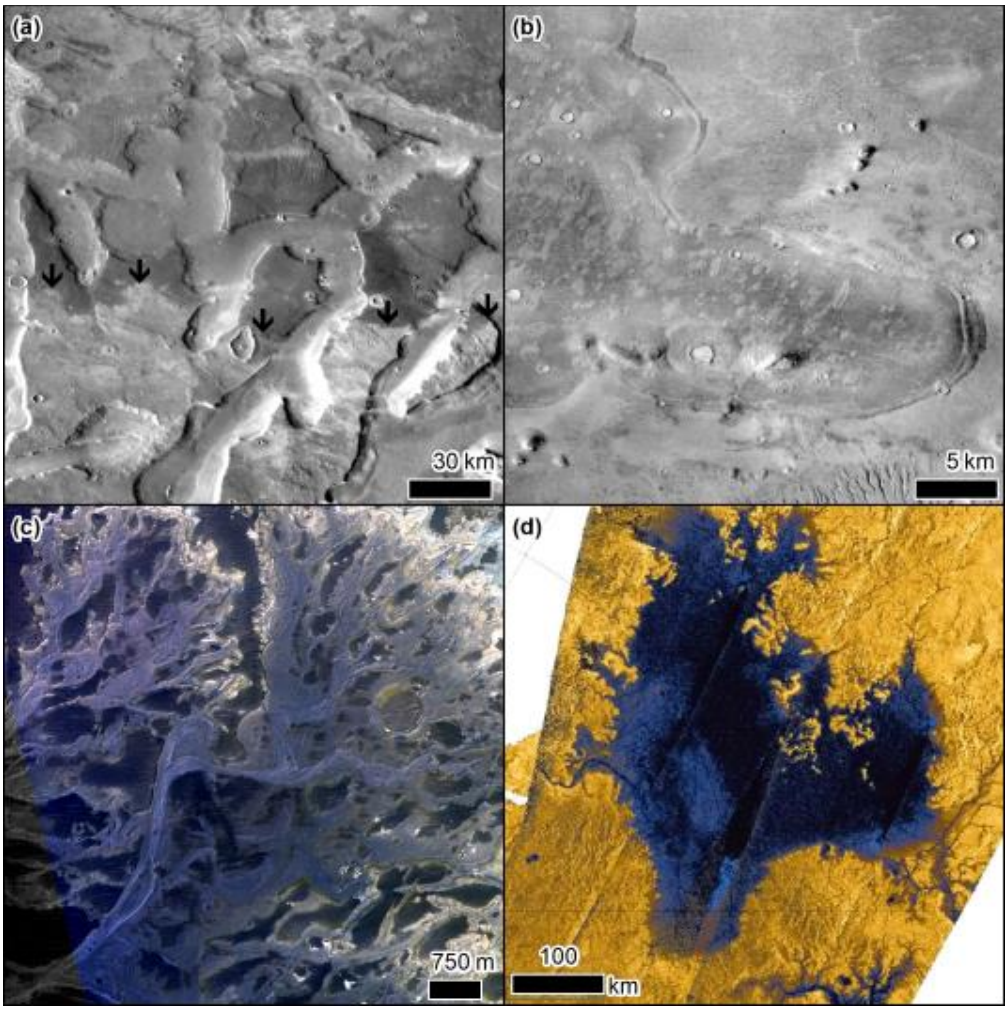

Figure 3: Coastal and lacustrine planetary landforms. a) Albedo contrast (black arrows) interpreted as a shoreline of a former norther ocean on Mars as seen in the Day IR THEMIS controlled mosaic available from the USGS (sunlight from the left). B) Lobate features interpreted to be tsunami runup deposits originating from an impact into a former norther ocean (sunlight from the left). CTX image P17_007835_2249, credit NASA/JPL/MSSS. c) CaSSIS false colour image of the inverted distributary channel systems within Eberswalde Crater on Mars, interpreted to be eroded remnants of a delta that formed within a lake in the crater (sunlight from bottom-right). CaSSIS images MY34_004384_206_1 and MY34_004384_206_2, credit ESA/Roscosmos/Unibe. d) Cassini false-colour radar image of Ligeia Mare, the second largest known sea of liquid hydrocarbons on Titan, credit: NASA/ESA/T. Cornet. North is up in all images.

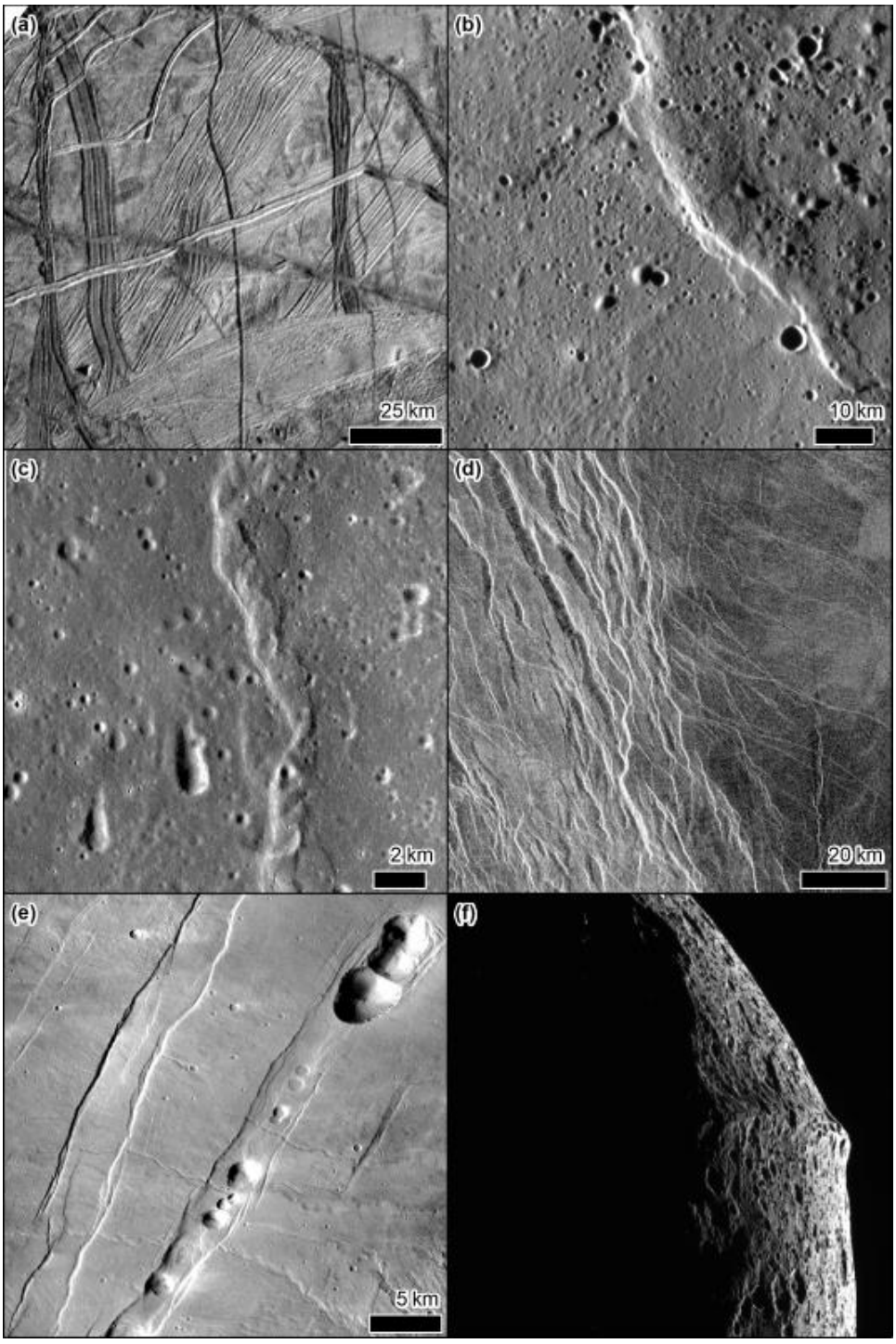

Figure 4: Tectonic planetary landforms. a) The surface of Europa divided into “plates” criss-crossed by fractures containing internal parallel ridges. Galileo SSI image 4700R, credit NASA/JPL-Caltech/SETI Institute. b) A lobate scarp on Mercury (sunlight from the left), MESSENGER MDIS NAC image EN1014447282M, credit NASA/Johns Hopkins University Applied Physics Laboratory/Carnegie Institution of Washington. c) Wrinkle ridge on the Moon (sunlight from the left), LROC NAC images M181023296 and M104376385, credit NASA/GSFC/ASU. d) Graben on Venus, extract of the Venus Magellan SAR FMAP Left Look Global Mosaic from the USGS. e) Graben and pit chains on Mars (sunlight from the left), CTX image B18_016700_2167, credit NASA/JPL/MSSS. f) Limb image of Iapetus, showing the 20 km high equatorial ridge, taken by Cassini N1568094172_2. North is up in all images except f.

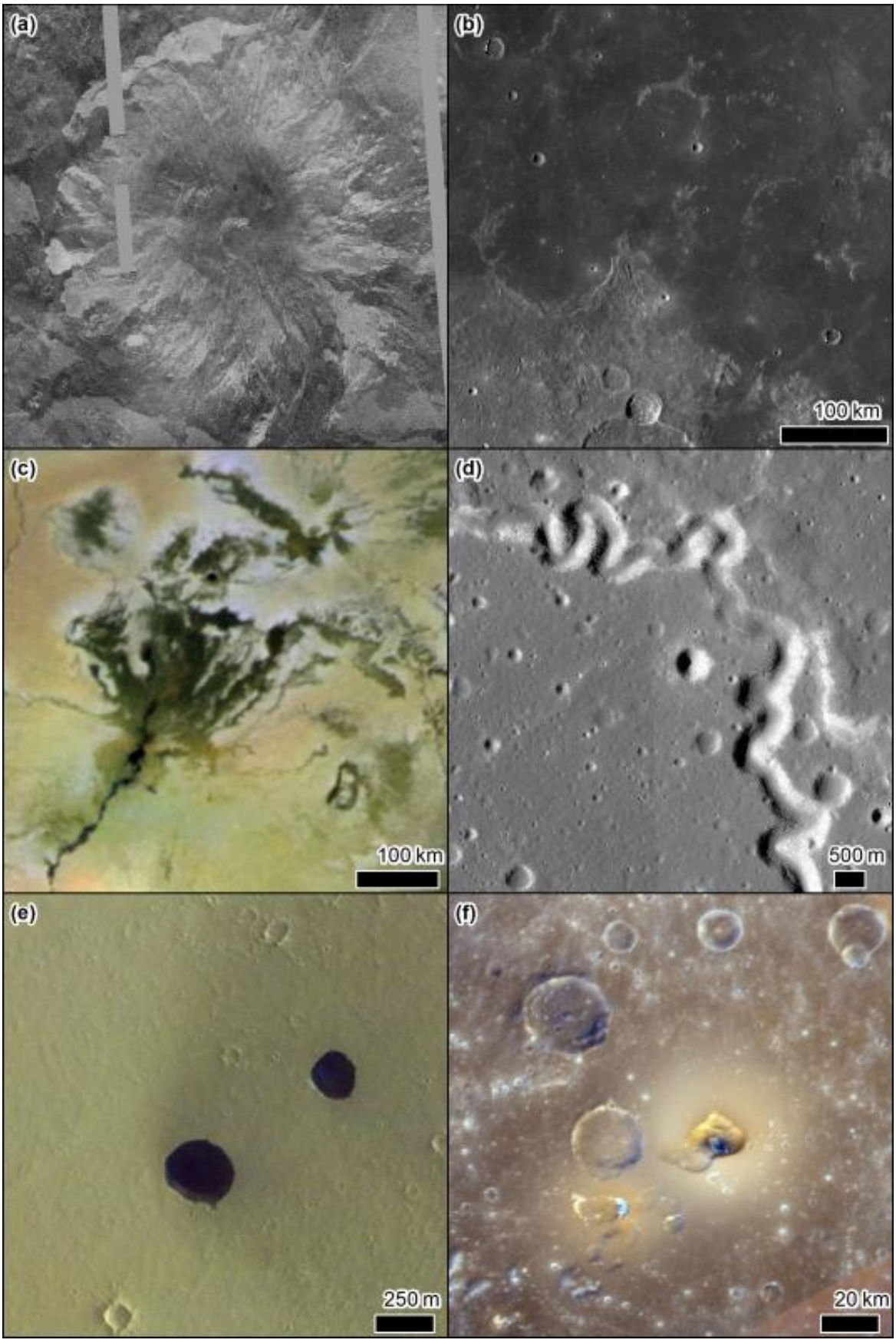

Figure 5: Volcanic planetary landforms. a) Tuulikki Mons a shield volcano on Venus, extract of the Venus Magellan SAR FMAP Left Look Global Mosaic from the USGS. b) The lunar maria with portions

of embayed impact crater rims visible and the contact with the highlands towards the bottom left (sunlight from the left). LORC WAC global mosaic made available by the USGS. c) Volund dark volcanic field on Io (Veeder et al., 2009)using the USGS Io basemap combining Voyager and Galileo images. d) Sinuous rilles on the Moon (sunlight from the left), LROC NAC image M1157998924, credit NASA/GSFC/ASU. e) Skylights on Mars (sunlight from the top-right), with the east-facing walls barely visible. CaSSIS false colour image MY36_015278_162_0, credit: ESA/Roscosmos/Unibe. f) Agwo Facula on Mercury, where the central vent is surrounded by smooth deposits with an orange coloration in the MDIS enhanced colour mosaic overlain by MDIS WAC image EW1012888774 (where sunlight is from the bottom), credit NASA/Johns Hopkins University Applied Physics Laboratory/Carnegie Institution of Washington. North is up in all images.

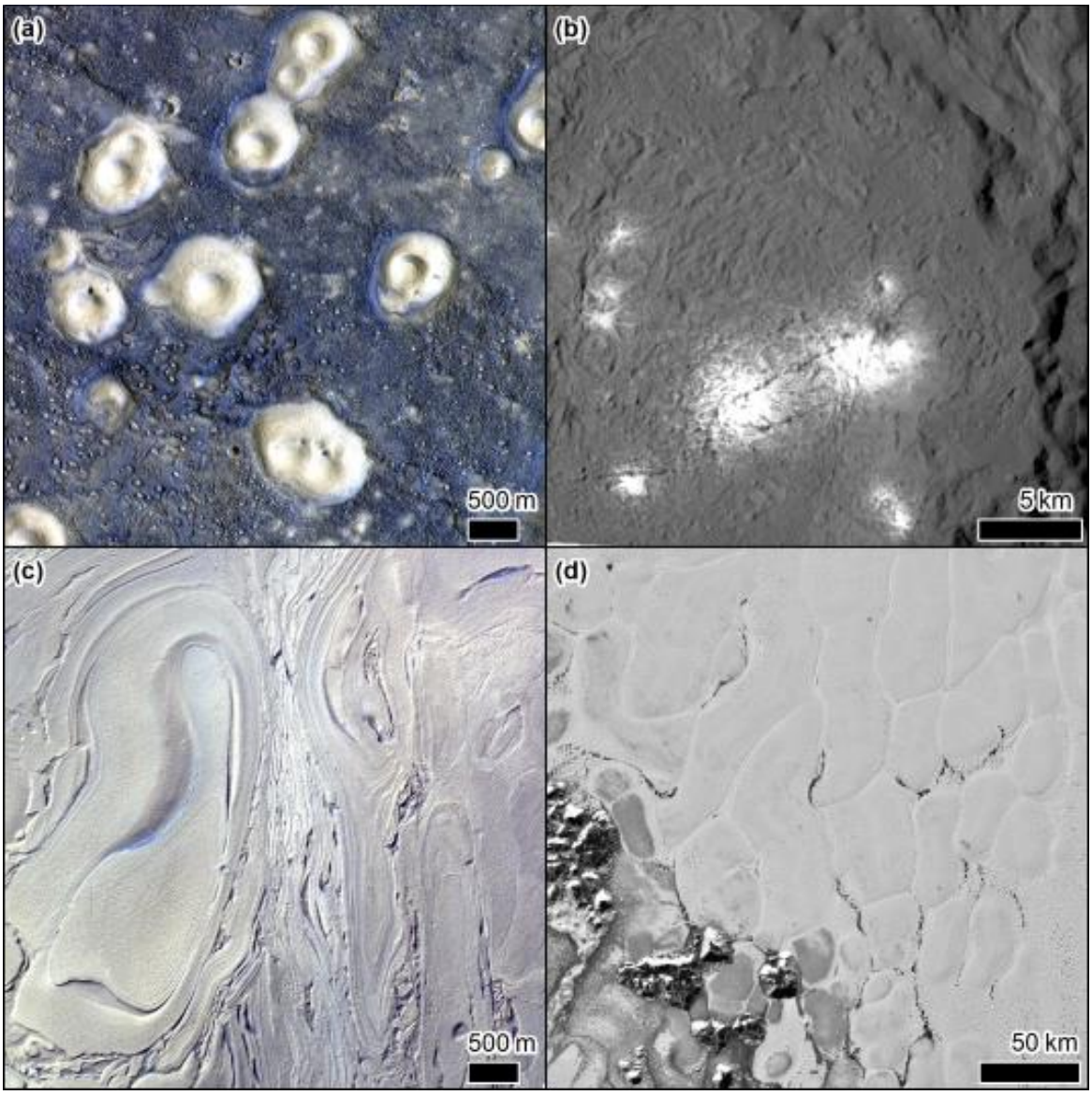

Figure 6: Sedimentary volcanism and cryo-volcanic landforms. a) Pitted cones interpreted to result from mud volcanism in Acidalia Planitia on Mars (sunlight from the top-right). CaSSIS image MY35_009227_048_0 credit: ESA/Roscosmos/Unibe. b) Bright faculae in Occator Crater on Ceres interpreted to be salt deposits resulting from cryovolcanism (sunlight from the right). DAWN framing camera image FC21B0070808_16169044543F6C, credit NASA/JPL-Caltech/UCLA/MPS/DLR/IDA. c) The enigmatic banded terrain on the floor of Hellas Basin on Mars (sunlight from the left). CaSSIS image MY36_015427_317_0 credit: ESA/Roscosmos/Unibe. d) The mysterious cellular structure of

Sputnik Planitia on Pluto (sunlight from the top), image New Horizons global mosaic from the USGS. North is up in all images.

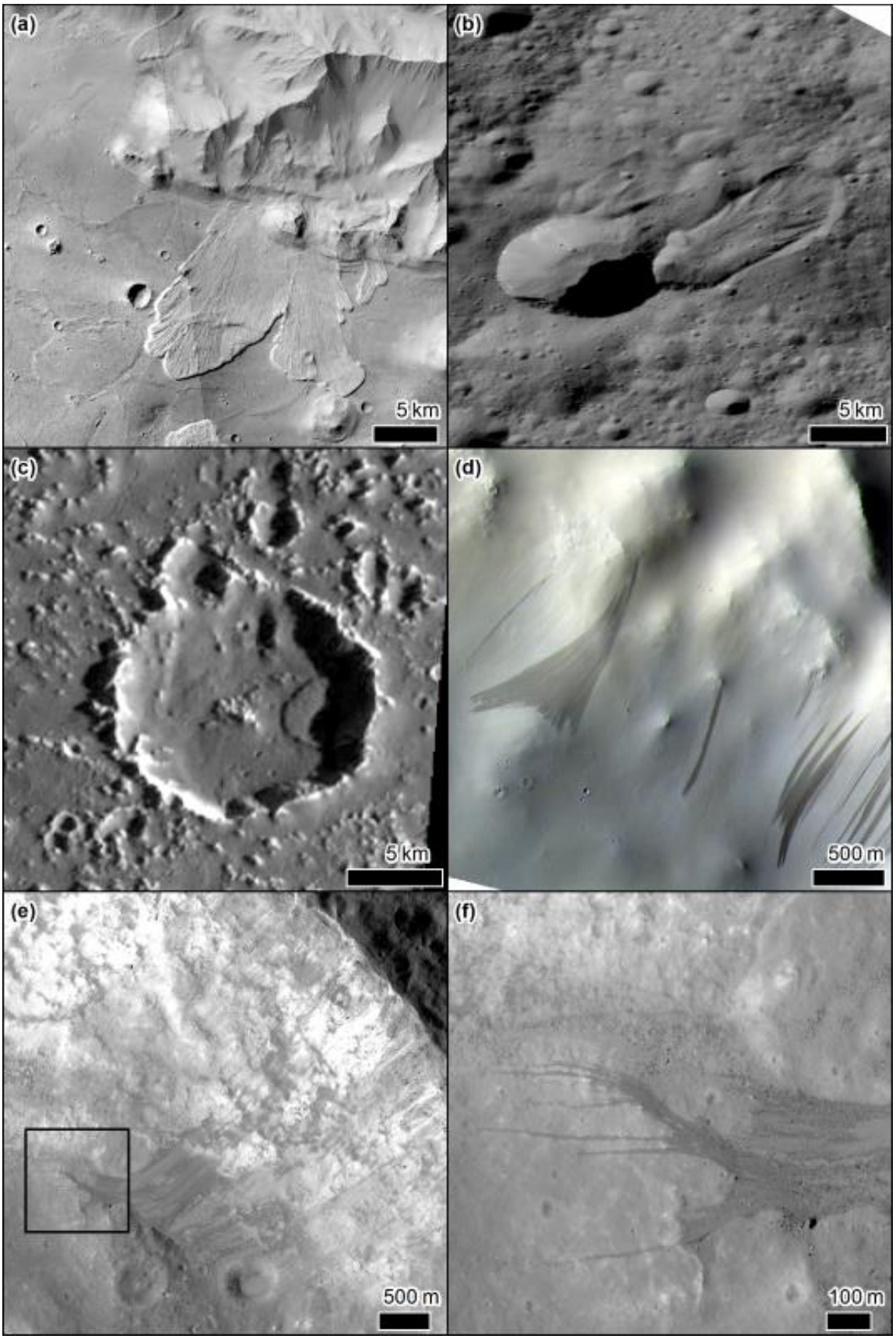

Figure 7: Planetary Mass Movements. a) Landslides in Valles Marineris on Mars (sunlight from the left), CTX images D20_034988_1669, G19_025850_1688, credit NASA/JPL/MSSS. b) Landslide on Ceres (sunlight from the bottom), DAWN FC FC21A0061028_16091125549F1D. c) Landslide on Callisto (sunlight from the right), Galileo SSI image 2840R, credit NASA/JPL-Caltech/SETI Institute. d)

Slope Streaks on Mars (sunlight from the left), CaSSIS image MY36_015392_011_0 credit: ESA/Roscosmos/Unibe. e) Granular flows in Kepler Crater on the Moon (sunlight from the left), LROC NAC images credit: NASA/GSFC/ASU. f) Zoom in on the termini of the granular flows in panel e. North is up in all images.

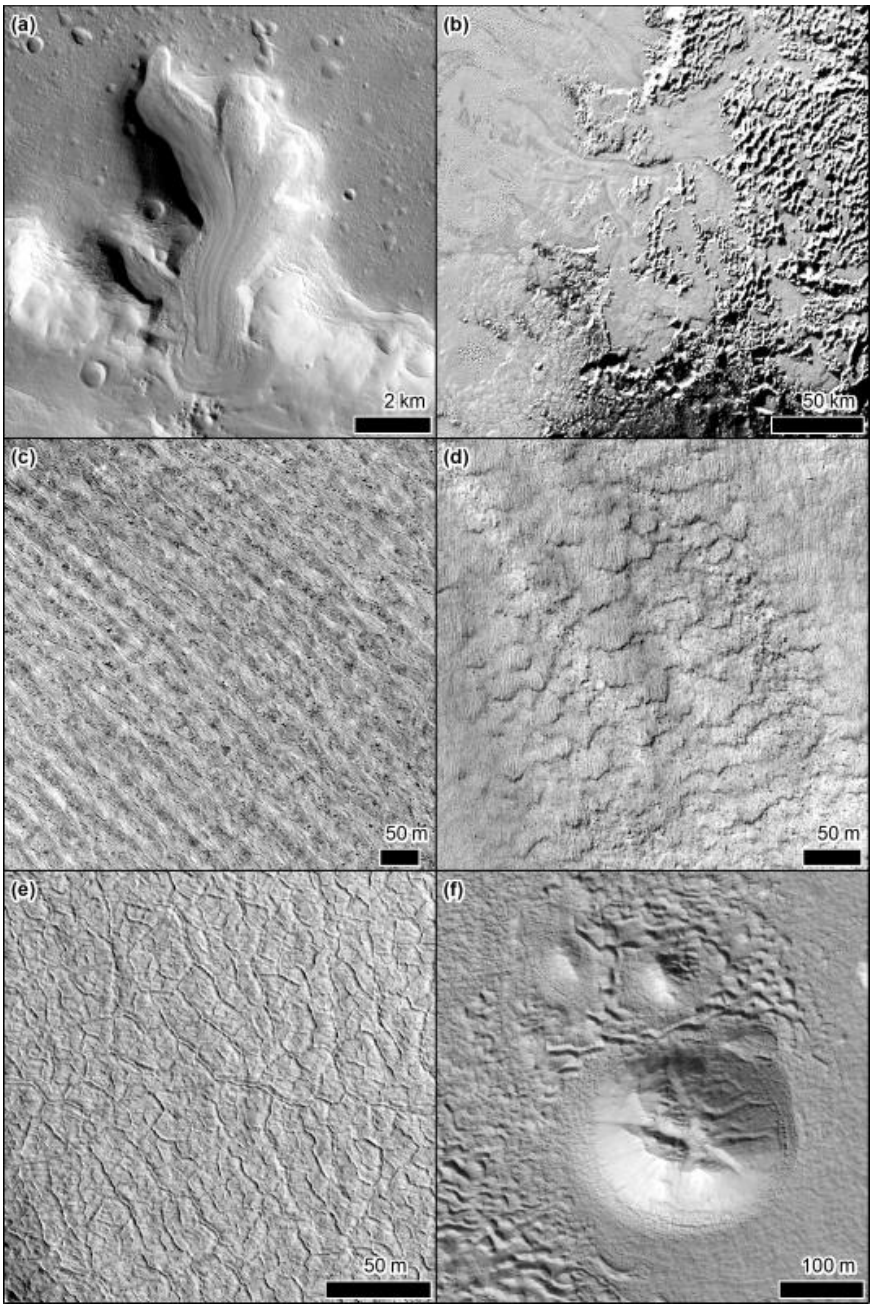

Figure 8: Planetary glacial and periglacial landforms. a) Debris covered glacier on Mars (sunlight from the left), CTX Image B05_011776_2208, credit NASA/JPL/MSSS. b) Glacial flows on Pluto imaged by New Horizons (sunlight from top-left), taken from the Global Mosaic available from the USGS. c) Linear arrangements of boulder propagating downslope interpreted to be sorted patterned ground on an impact crater wall in the high northern latitudes on Mars (sunlight from top-left), HiRISE image PSP_009580_2485, credit NASA/JPL/UofA. d) Lobate forms on the wall of an impact crater on Mars interpreted to be solifluction lobes (sunlight from the left), HiRISE image ESP_023679_1365, credit NASA/JPL/UofA. e) Polygonal fractured ground where the polygon boundaries are raised as single or double ridges, termed low centres polygons (sunlight from bottom-left), HiRISE image

PSP_005821_1095 credit NASA/JPL/UofA. f) A mound with a fractured summit near Moreaux Crater on Mars interpreted to be a pingo (sunlight from bottom-left), HiRISE image ESP_058140_2225 credit NASA/JPL/UofA. North is up in all images.

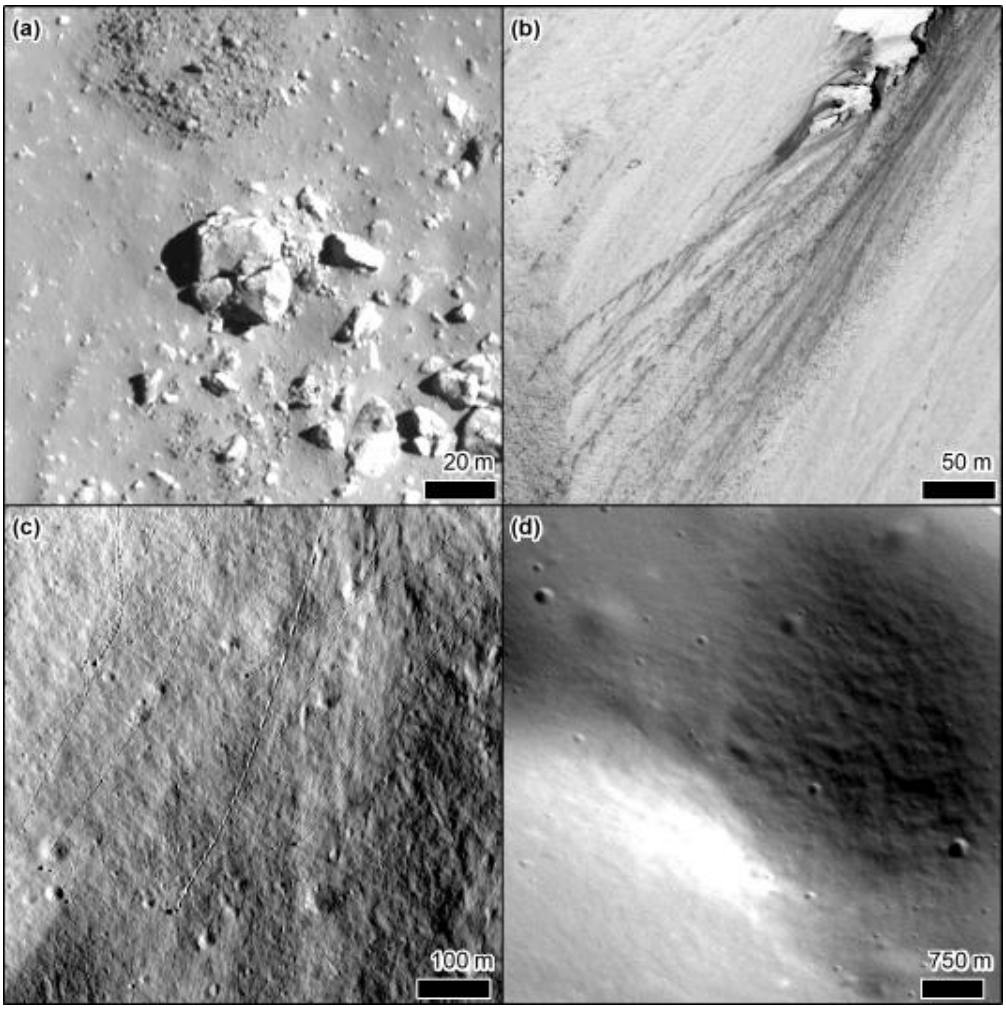

Figure 9: Weathering on planetary surfaces. a) Fractured rocks around Byrgius A Crater on the Moon (sunlight from the right), LROC NAC image M175698856LE, credit NASA/GSFC/ASU. b) Tracks and low albedo "ejecta" left by recent rockfalls on a crater wall on Mars (sunlight from the left), HiRISE image PSP_004110_1640, credit NASA/JPL/UofA. c) Multiple rocks which have left depressions behind them while rolling and bouncing over the lunar surface (sunlight from the right), LROC NAC image M1198659818LE, credit NASA/GSFC/ASU. d) Undulating, irregular surface texture on Mercury (sunlight from the bottom-left), termed "Elephant hide" (Zharkova et al., 2020) MDIS NAC image EN1042186062M, credit NASA/Johns Hopkins University Applied Physics Laboratory/Carnegie Institution of Washington. North is up in all images.

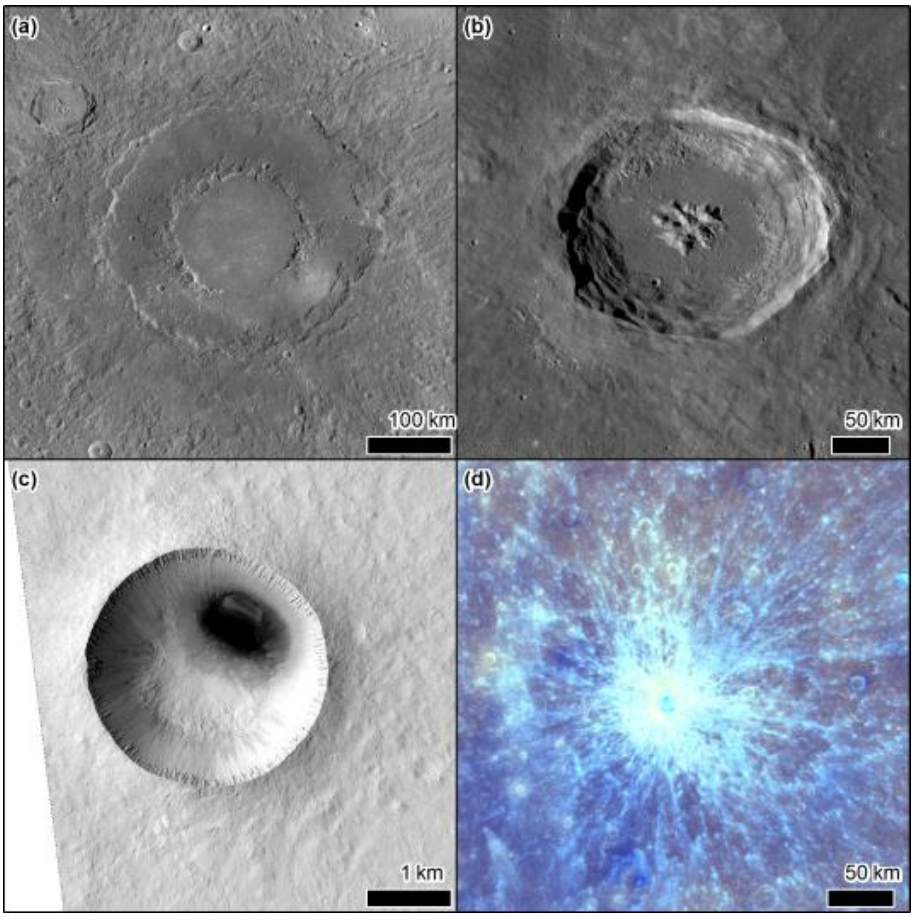

Figure 10: Impact craters on Planetary bodies. a) Rachmanioff, an impact basin on Mercury, with noticeable multiple rings (sunlight from the right), MDIS global BDR mosaic, credit NASA/Johns Hopkins University Applied Physics Laboratory/Carnegie Institution of Washington. b) Arstillus, a complex crater with central peak and wall terraces on the Moon (sunlight from the left), LRO global WAC mosaic, credit NASA/GSFC/Arizona State University. c) ~ 2km diameter simple crater on the floor of Pasteur Crater on Mars (sunlight from the left), HiRISE image ESP_045152_2000, credit NASA/JPL/UofA. d) Petipa, an impact crater with rayed ejecta on Mercury (sunlight from overhead), MDIS global enhanced color mosaic, credit NASA/Johns Hopkins University Applied Physics Laboratory/Carnegie Institution of Washington. North is up in all images.

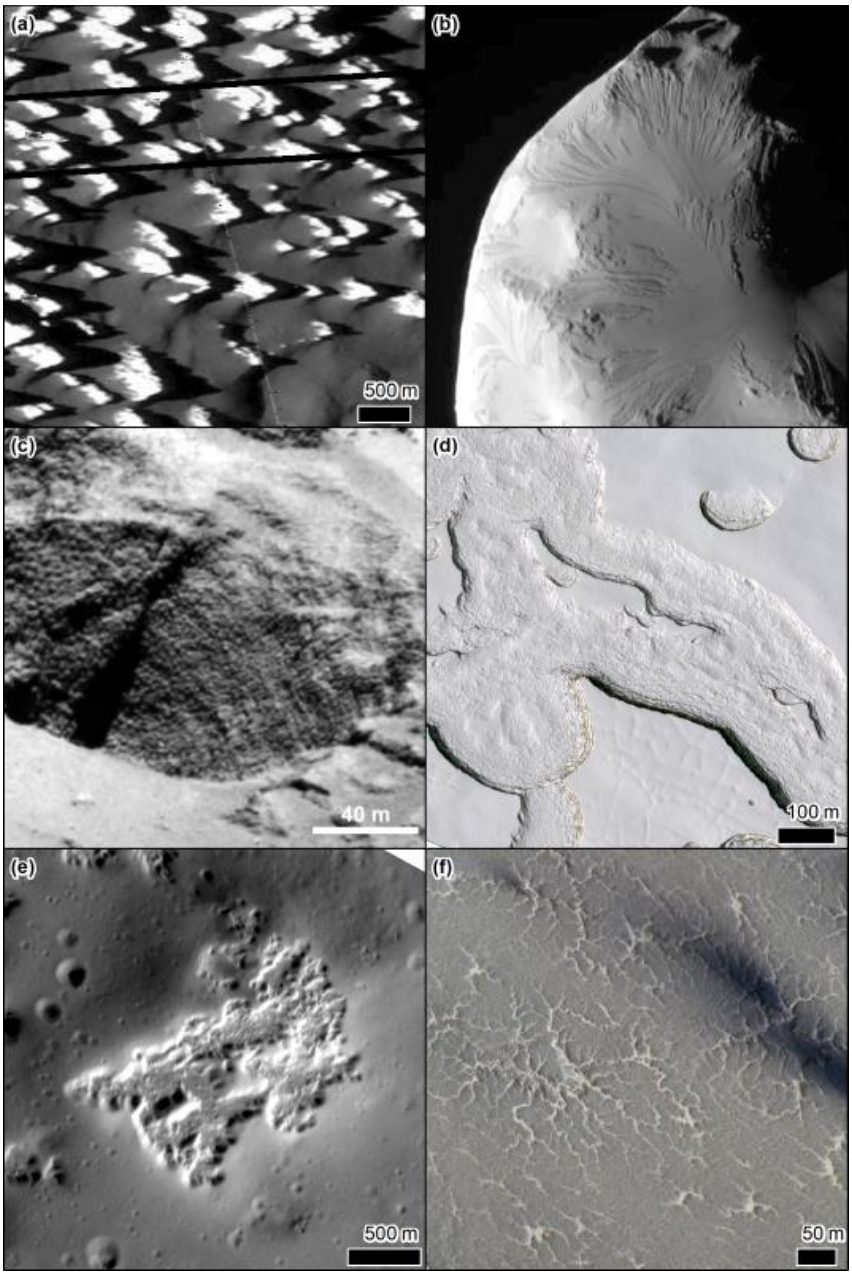

Figure 11: Sublimation dominated landscapes and landforms. a) Pinnacle terrain on Callisto Galileo (sunlight from the left) SSI image 5214R, credit NASA/JPL-Caltech/SETI Institute. b) Image of the surface of Helene a moon of Saturn (sunlight from the left) taken by the Cassini spacecraft image reference N1687119876_1, credit NASA/JPL-Caltech/ASI, scene is about 30 km across. c) Oblique image of the wall of a steep pit revealing internal structure (sunlight from the left), on comet 67P/Churyumov–Gerasimenko taken by the OSIRIS narrow-angle camera, credit ESA/Rosetta/MPS for OSIRIS Team MPS/UPD/LAM/IAA/SSO/INTA/UPM/DASP/IDA. d) Siss cheese terrain in the CO_2 ice on the south polar cap of Mars (sunlight from the bottom-left), HiRISE image ESP_057828_0930, credit NASA/JPL/UofA. e) Hollows on Mercury (sunlight from the bottom-right), MDIS NAC image EN1042186062M, credit NASA/Johns Hopkins University Applied Physics Laboratory/Carnegie Institution of Washington. f) Spiders on Mars (sunlight from the top-right), where the dark marks are dust fans deposited by seasonal jets, HiRISE image ESP_055604_0930, credit NASA/JPL/UofA.